

A geometric approach to understand biological responses to environmental fluctuations from the perspective of marine organisms

Gimenez Noya, Luis

Marine Ecology Progress Series

DOI:
[10.3354/meps14414](https://doi.org/10.3354/meps14414)

Published: 19/10/2023

Peer reviewed version

[Cyswllt i'r cyhoeddiad / Link to publication](#)

Dyfyniad o'r fersiwn a gyhoeddwyd / Citation for published version (APA):
Gimenez Noya, L. (2023). A geometric approach to understand biological responses to environmental fluctuations from the perspective of marine organisms. *Marine Ecology Progress Series*, 721, 17-38. <https://doi.org/10.3354/meps14414>

Hawliau Cyffredinol / General rights

Copyright and moral rights for the publications made accessible in the public portal are retained by the authors and/or other copyright owners and it is a condition of accessing publications that users recognise and abide by the legal requirements associated with these rights.

- Users may download and print one copy of any publication from the public portal for the purpose of private study or research.
- You may not further distribute the material or use it for any profit-making activity or commercial gain
- You may freely distribute the URL identifying the publication in the public portal ?

Take down policy

If you believe that this document breaches copyright please contact us providing details, and we will remove access to the work immediately and investigate your claim.

1 **A geometric approach to understand biological responses to environmental fluctuations**
2 **from the perspective of marine organisms**

3 Luis Giménez^{1,2,*}

4 1. School of Ocean Sciences, Bangor University, LL59 5AB , Anglesey UK

5 2. Alfred-Wegener-Institut, Helmholtz-Zentrum für Polar- und Meeresforschung,
6 Biologische Anstalt Helgoland, 27498 Helgoland, Germany

7

8 *Corresponding author: Luis Giménez: School of Ocean Sciences, Bangor University, LL59
9 5AB , Anglesey UK

10

11

12

13 Running title: Responses of marine biological systems environmental fluctuations

14

15

16

17

18

19

20

21

22

23

24

25

26 **Abstract**

27 A main concern in marine ecology is understanding the mechanisms driving responses of
28 biological systems to environmental fluctuations. A major issue is that each biological system
29 (e.g. organism, ecosystem) experiences fluctuations according to its own intrinsic
30 characteristics. For instance, how an organism experiences a thermal fluctuation, i.e as a long
31 marine heatwave or as a mild pulse, depends on its thermal tolerance and developmental time,
32 which can vary as the fluctuation is experienced. Here, I explore a geometric approach,
33 considering the biological perspective. Environmental fluctuations are represented as points in
34 a “space of fluctuations”. The biological perspective is then defined as a coordinate frame
35 within that space. Coordinates are given by components (e.g. amplitude and time scale)
36 characterising each environmental fluctuation, which are then transformed into biological
37 scales, using biological traits (tolerance and biological time). Using simulations of organisms
38 growing under thermal fluctuations with different characteristics, I show how this approach:
39 (1) Enables to integrate physiology and phenology to better interpret biological responses to
40 fluctuating environments. (2) Improves understanding of the role of adaptive plasticity as a
41 rescue effect. (3) Facilitates understanding the effects of thermal fluctuations on additional
42 organismal traits (e.g. body mass). I also discuss wider applications in the context of species
43 persistence, coexistence, biodiversity, and ecosystem function in scenarios of extreme
44 fluctuations.

45

46

47

48

49

50

51 **Keywords:** acclimation, fluctuating environments, marine heatwaves, multiple stressors,
52 phenology, phenotypic plasticity, thermal tolerance

53

54

55

1. INTRODUCTION

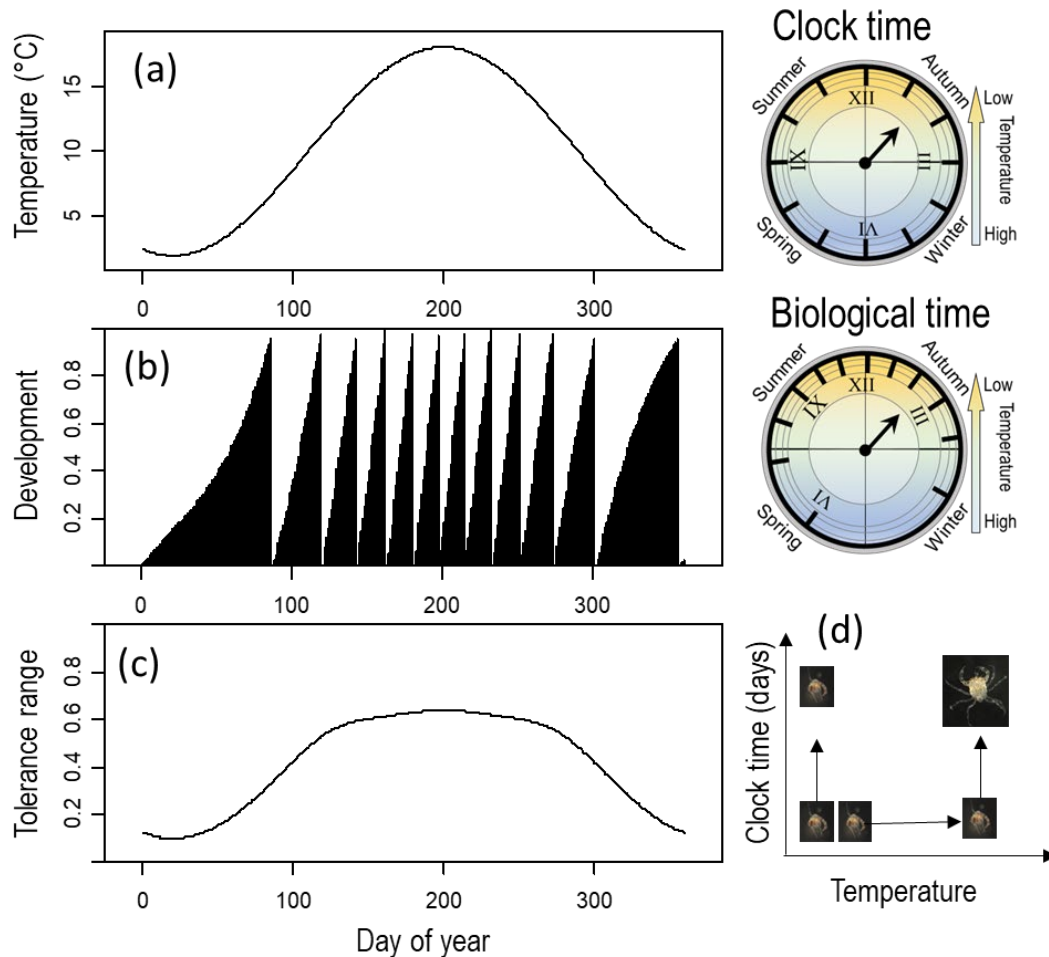
56 One of the biggest challenges in marine ecology is understanding mechanisms driving
57 responses of biological systems to environmental fluctuations (Thompson et al. 2013, Kroeker
58 et al. 2020, Gerhard et al. 2023). Environmental fluctuations occur at several time scales
59 (Chave 2013) and extreme fluctuations have increased over the past decades. For instance,
60 marine and atmospheric heatwaves of period ranging from days to months have become more
61 frequent, more extreme, and less coherent in the past 30 years (Russo et al. 2015, Hobday et
62 al. 2016, Benedetti-Cecchi 2021). Ecologists are aware that fluctuating environments can drive
63 biological systems through mechanisms that differ from those present in constant environments
64 (Levins 1968, Sæther, B.-E. & Engen 2015, Denny 2019, Bernhardt et al. 2020). However, our
65 mechanistic understanding of responses to environmental fluctuations is limited because most
66 experiments are using static designs, i.e. manipulating an environmental variable but keeping
67 each treatment level constant over time. Results from experiments with static designs do not
68 correctly predict responses to fluctuating conditions. For instance, adaptive plasticity evolves
69 strictly in fluctuating environments (Scheiner 2016); at the organismal level, adaptive plasticity
70 may be triggered by a fluctuation after some environmental threshold is surpassed, but not
71 necessarily if the average condition of the fluctuation is experienced. Above a threshold,
72 important (or irreversible) damage, may lead to carry-over effects (Minuti et al 2022). At the
73 population and community level, responses to mean conditions differ to those from extremes
74 (Lynch et al. 2014). At the community level, fluctuations drive historical/legacy effects
75 associated to the time scale of recovery time between fluctuations (Williams et al. 2011, Dal
76 Bello et al. 2017). Storage effects and relative non-linearity are mechanisms sustaining species
77 coexistence that operate strictly in fluctuating environments (Chesson 2018). Hence, in many
78 cases we cannot use the information provided by most static experiments even if they represent
79 the average condition of the fluctuation.

80 We need experiments manipulating the components characterising the fluctuations. Fluctuation
81 components may be defined as the amplitude, average, maximum, minimum, time scale, and
82 timing of a fluctuation (Jentsch et al. 2007, Gunderson et al. 2016, Donelson et al. 2018,
83 Giménez et al. 2022). In the case of noise, such components may be defined as the intensity
84 and the dominating frequency (Vasseur & Yodzis 2004), which have ecological and
85 evolutionary consequences (Romero-Mujalli et al. 2021). Experiments provide mechanistic
86 understanding (Benedetti-Cecchi 2003, 2006, Koussoropolis et a. 2017, Gunderson et al. 2016,
87 Boyd et al, 2018, Gerhard et al. 2023) and are needed as a part of a wider set of methodologies

88 (Dawson et al. 2011, Thompson et al. 2013, Koussoropolis et al. 2017). The experimental study
89 of effects of fluctuations on biological systems brings both logistical and conceptual challenges
90 (Thompson et al. 2013, Giménez et al. 2021, 2022). Logistical challenges associated with the
91 number of replications, have been addressed through specific experimental designs (Boyd et
92 al. 2018, Kreyling et al. 2018). Issues associated with teasing apart the role of different
93 components characterising a fluctuation have also been addressed in the case of disturbance
94 events, with intensive effort into separating the effect of mean and temporal variance of a
95 fluctuation (Benedetti-Cecchi 2003, 2006, Bertocci et al. 2005, 2007, Maggi et al. 2012).

96 In recent years there has been an intensive effort to generate a general framework to incorporate
97 fluctuations into studies of effects of climate change on organisms (Gunderson et al. 2016,
98 Boyd et al. 2018, Gerhard et al. 2023). Within the framework, a major gap is the consideration
99 of organismal perspective (Jackson et al. 2021), given by how biological systems experience a
100 fluctuation in relation to their own biological traits. The importance of studying effects of
101 environmental fluctuations on biological traits is obvious and has been widely recognised. We
102 can therefore use current information on critical biological traits, to develop a mathematical
103 foundation and provide metrics to quantify fluctuation components, from the organismal
104 perspective. For instance, recent studies have quantified the time scales of thermal fluctuations
105 using biological time as a trait (time to metamorphosis: Giménez et al. 2022; generation time:
106 Munch et al 2023). Some important facts (Fig. 1) motivating this approach are: (1) Biological
107 time scales, such as generation time (or time to reproduction) are central traits with direct
108 impact on fitness (Stearns 1986, chap. 6, Angilleta 2009, chap. 6). (2) Adaptive responses,
109 driving to evolutionary rescue (Chevin et al. 2010), can vary with time scales ranging from
110 short term plasticity (hardening) through acclimation to trans-generational plasticity and
111 genetic adaptation (Gerken et al. 2015, Donelson et al. 2018). (3) In ectotherms, within species,
112 increased temperature results in (a) strong non-linear effect on biological time through changes
113 in metabolic rates (Gillooly, et al. 2002, Rombough 2003, Giménez 2011), (b) increases in
114 aging rate (Burraco et al. 2020, Cayuela et al. 2021), and (c) increases in the speed of
115 behavioural responses (kinetic effects of temperature on behaviour: Abram et al. 2017).
116 Because in ectotherms, the above changes are the result of increases in kinetic energy within
117 cells and tissues, it is likely that changes in environmental temperature also affects the time
118 scale of adaptive plastic responses. Studies of the effects of temperature on biological time
119 have shown that: (1) Whether multiple-stressor responses are additive or interactive depends
120 on whether time is measured in “clock” vs biological units (Giménez et al 2022); this also

121 extends to how sensitive organisms are to a given stressor. (2) Re-scaling the equations of
 122 population dynamics to biological time, lead to more robust predictions of dynamics of
 123 ectotherms in seasonal environments (Munch et al 2023).



124

125 Figure 1. Simulated example of responses to thermal fluctuations in a marine ectotherm
 126 developing through 12 stages. (a) A seasonal thermal fluctuation and associated clock time
 127 where each of the clock 12 divisions represents a month and the colour gradient represents the
 128 temperature (for simplicity XII corresponds to the day of year of peak temperature). (b)
 129 Biological time: the cumulative proportion of development calculated as the proportion of
 130 development to each stage, using degree days (i.e. a stage is completed when the cumulative
 131 temperature reaches 280 °C days). Once a stage is reached, the cumulative proportion resets to
 132 zero and increases until a new stage is reached. In the associated biological clock, the position
 133 of the stages varies depending on temperature. Hence, the time marks in the biological and
 134 clock do not coincide. (c) Thermal fluctuation as experienced from the organism, calculated as
 135 the proportion of the upper thermal range (from the optimum to the upper thermal tolerance
 136 limit). The pattern of fluctuation is buffered with respect to the pattern in (a) because organisms
 137 acclimate to high temperature over the summer. (d) Illustration of an experiment where two
 138 sibling crab larvae are reared at different temperatures for a fixed amount ~~to~~ of clock time, after
 139 which the sibling exposed to higher temperature is developmentally older than the one reared
 140 at low temperature. In (d) photographs by the author.

141 Because system experience must be multifactorial (i.e. depending on biological time plus other
142 traits), we need a framework that consider additional traits as metrics of other fluctuation
143 components. Hence, in this paper, I expand a previous framework, explored in Giménez et al.
144 (2022), which did not consider a biological metric for the magnitude (e.g. intensity, amplitude,
145 average) of an environmental fluctuation. A biological metric for fluctuation magnitude is
146 critical for example to categorise a given fluctuation as an “extreme event”. This is relevant for
147 instance in the context of the study of heatwaves, where definitions may be based on
148 climatology or biology (Bailey & van de Pol 2015) and on different references or baselines
149 against which fluctuations are compared (e.g. Hobday et al. 2016, Jacox 2019). We also need
150 to account for intra and interspecific effects of environmental fluctuations and the associated
151 mechanisms. Within species, tolerance is shaped by both adaptive (i.e. adaptive plasticity and
152 genetic evolution: Donelson et al. 2018) and non-adaptive responses (e.g. carry-over effects
153 and “silver spoon” maternal effects: Pechenik 2006, Uller et al. 2013, Ruiz-Herrera 2017).
154 Mechanisms underpinning tolerance also occur at other levels of organization: populations may
155 differ in their gene frequencies which drive portfolio effects (Schindler et al. 2015, Šargač et
156 al. 2022) and communities differ in the species composition driving species complementarity
157 (Cadotte et al. 2013), all acting as compensatory mechanisms. In those situations, tolerance
158 should vary over time as a fluctuation is experienced. In synthesis, organismal experience (or
159 that existing at other levels of organization) can be quantified as tolerance and biological time
160 and is characterised by complex dynamics, which shape other biological responses.

161 The approach proposed here (thereafter called “space of fluctuations approach”, abbreviated as
162 “SOFiA”), incorporates the perspective of the biological system in understanding biological
163 responses to fluctuations. This is based on the idea (borrowed from differential geometry and
164 physics: see e.g. Needham 2021) that there is no “absolute” perspective to characterise a
165 fluctuation and its components; instead, there are different perspectives, from different systems
166 (e.g. the human observer and an organism experiencing the fluctuation). This paper is
167 structured as follows: First, I present SOFiA in a wider context aimed at making predictions of
168 responses, given field-observed environmental fluctuations. Second, I present the core ideas
169 (space of fluctuations and coordinate frames to quantify the organismal perspective). Third, I
170 explore SOFiA using three cases at the organismal level. Fourth, I use a worked example of a
171 simulated factorial experiment, manipulating fluctuation components to clarify the design and
172 data needed to quantify the organismal perspective. My emphasis is on effects of thermal

173 fluctuations at the organismal level, but wider applications, on populations and ecosystems, are
174 presented in the Discussion.

175 **2. METHOD CONTEXT**

176 The approach proposed here must be viewed as integrated into a wider framework (Fig. 2)
177 combining field observations, experiments, and models predicting responses of biological
178 systems to multiple fluctuating environmental drivers (Denny et al. 2009, Dawson et al. 2011,
179 Koussoroplis et al. 2017, Gerhard et al. 2023). Thermal fluctuations (e.g. a heatwave) are
180 characterised by a set of components, e.g. time scale, amplitude, cumulative intensity, rates of
181 increase and decrease in temperature (see e.g. Hobday et al. 2016 for marine heatwaves). Field
182 observations provide information on the range of fluctuation types (characterised by their
183 components) that are then used to define the range of values considered in an experiment. The
184 effects of thermal fluctuations are quantified using factorial-orthogonal experiments, teasing
185 apart the effect of each component. The output of the experiment can then be used for
186 predictions in the field or for parameterization of models (Fig. 2). Predictions in the field may
187 be based, for instance, on scale transition theory, a method providing estimations of average
188 responses from mean, variances and covariances of environmental variables (see worked
189 example, Chesson 2012, Denny & Benedetti-Cecchi 2012, Dowd et al. 2015, Koussoroplis et
190 al. 2017).

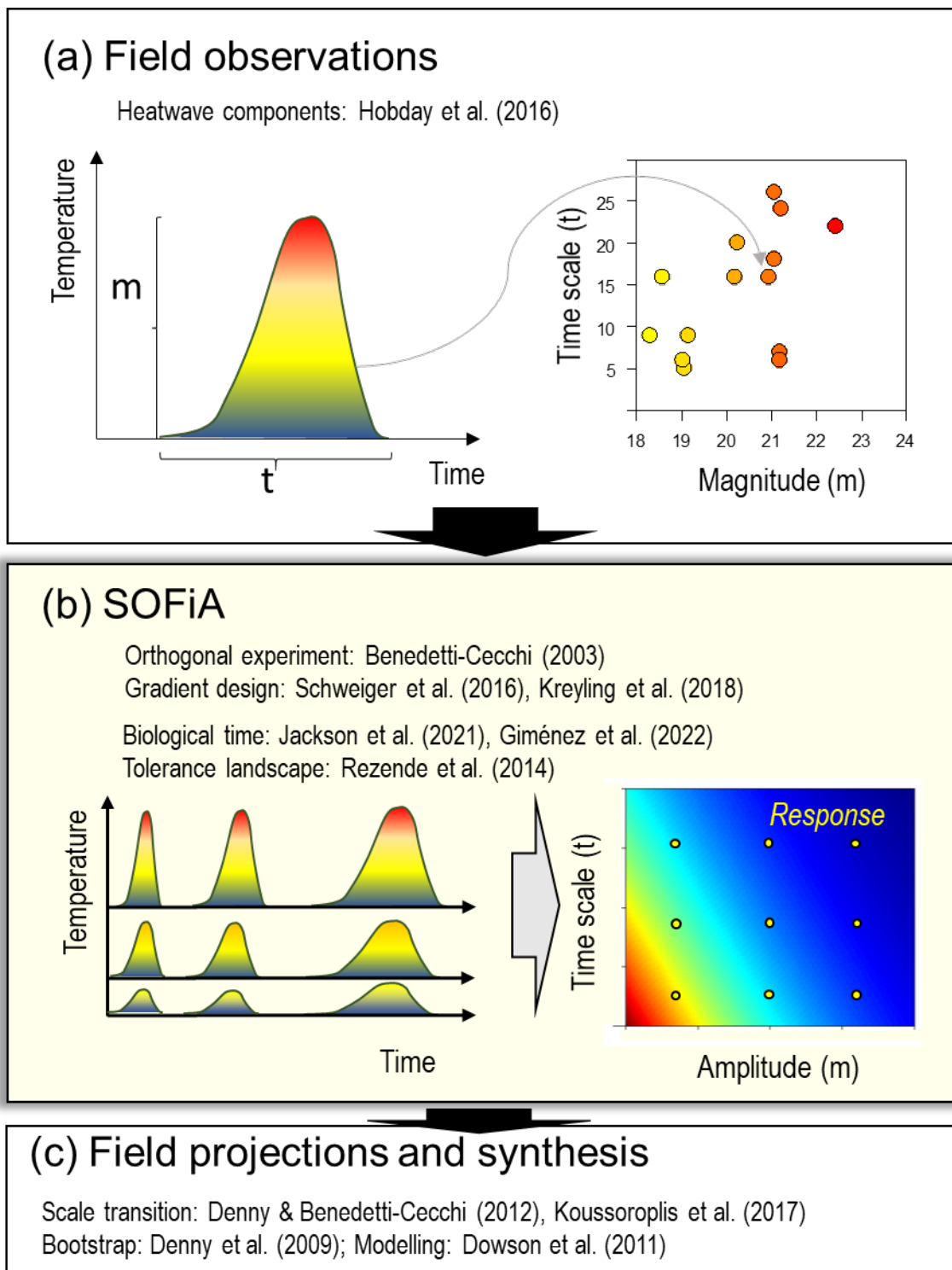
191 **2.1 Experimental designs**

192 The central point in SOFiA concerns the experimental phase: Orthogonal experiments are
193 necessary to derive quantitative relationships between predictors and responses and are
194 essential for the development of mechanistic models (Benedetti-Cecchi 2003). This argument
195 is valid also when different environmental variables (or fluctuation components) co-vary in the
196 field. In such a case, the experiment will provide information that is relevant to current
197 environmental context, enable predictions of future scenarios where the covariation is broken
198 (Benedetti-Cecchi 2003, Boyd et al. 2018) and cover for responses to rare events (Kreyling et
199 al. 2014) such as extreme heatwaves. One may envisage an orthogonal experiment, considering
200 fluctuations components as “fixed” predictors (then analysed with e.g. ANOVA) or as
201 continuous predictors. The latter method is more appropriate for the approach presented here;
202 it can be based on surface response designs (Box & Wilson 1951, Cottingham et al. 2005,
203 Thompson et al. 2013, Kreyling et al. 2014, 2018, Schweiger et al. 2016).

204 Surface response designs will capture non-linear and non-additive responses to the fluctuation
205 components present in the data. Because those responses are common in ecology and evolution
206 (Levin 1998, Ruel & Ayres 1999, Schaffer 2009, Gunderson et al. 2016, Kroeker et al. 2020)
207 surface response designs are better suited to improve ecological models than the ANOVA type
208 design (except when the predictor in question is categorical). Surface response designs also
209 provide the appropriate response function needed in scale transition theory, developed to
210 incorporate interactive and non-linear responses to environmental fluctuations (Koussoroplis
211 et al. 2017).

212 The main issue with surface response designs is the large number of experimental units needed
213 to cover the predictor space defined by the fluctuation components. For example, consider an
214 experiment with two components and a maximum of 90 replicate units; 10 replicate units per
215 treatment combination would constraint the experiments to 9 locations (i.e. 3x3 combinations
216 of component values) in the predictor space. A potential solution is to use sequential
217 experiments covering different regions of the predictor space at each stage (Box & Wilson
218 1951); this may be problematic if replicates are likely to vary in time for some reason other
219 than the experimental random variation. An alternative solution is to either optimise the number
220 of replicates or to use un-replicated designs, a technique known as “gradient analysis”
221 (Kreyling et al. 2018); for instance, at 90 replicate units, one may define 90 locations (as a 9x10
222 grid), allocating one unit each. Modelling exercises show that designs with low or no
223 replication, but many locations, outperform replicated designs with fewer locations in detecting
224 non-linear responses (Schweiger et al. 2016, Kreyling et al. 2018).

225



226

227 Figure 2. SOFiA in the wider context of scaling experiments to predictions under field
 228 conditions. (a) Thermal fluctuations (e.g. heatwaves) vary considerably in amplitude (m) and
 229 time scale (t). (b) In SOFiA, an orthogonal experiment is carried out simulating fluctuations of
 230 different combinations of m and t ; a response (e.g., body size as a heat map, with values
 231 decreased from red to blue) is quantified, at fixed locations (some represented as yellow
 232 points). In addition, organismal traits are used as metric to define coordinate frames where the
 233 additional biological responses are quantified. (c) Experimental results are used together with
 234 field data for models, projections (i.e. scenario analysis) or predictions. The references cited
 235 show the literature providing ideas concerning one or more steps.

236 **2.2 Fluctuation components**

237 We need an approach accounting for historical effects found at different levels of organization.
238 For instance, at the organismal level, acclimation, and carry-over stress effects, are pervasive
239 (Giménez 2006, 2020, Pechenik 2006, Marshall et al. 2016), and can drive recruitment in
240 marine populations (Torres et al. 2016). Historical effects are also important at the community
241 level and their evaluation requires the consideration of time scales explicitly in the design (e.g.
242 see Dal Bello et al. 2017).

243 In the approach proposed here (Fig. 2b) fluctuations are characterised by an explicit time
244 variable in addition to a magnitude variable (if only two components are considered). The use
245 of the time variable enables to capture any historical effect in addition to rescale responses in
246 biological time (see section of worked example, Giménez et al. 2022). The use of a time
247 variable helps to move away from estimations of tolerance based keeping organisms at constant
248 conditions or using ramp experiments that do not necessarily match the time scale of natural
249 environmental fluctuations (Terblanche et al. 2011, Rezende & Santos 2012, Gunderson et al.
250 2016). The choice of the magnitude variable depends on the situation; I focus on the amplitude,
251 to account for cases where historical responses are associated to threshold phenomena (e.g.
252 acclimation being triggered after some temperature level is experienced). In the field, time
253 scales and amplitudes of fluctuations can be estimated through direct observations or from
254 statistical models such as Fourier analysis or polynomial fitting. In this set up, projections or
255 predictions (see worked example) would be based on a response function matching the time
256 scale of field-observed fluctuations.

257

258 **3. THE SPACE OF FLUCTUATIONS**

259 **3.1 Coordinate frames**

260 The central concept of SOFiA is that environmental fluctuations are characterised by a set of
261 components and represented as points in a space. This multidimensional space resembles the
262 one defined in multivariate analysis such as principal component analysis (or any other
263 extension), where the principal components constitute a coordinate frame (Legendre &
264 Legendre 1998). The space of fluctuations has also similarities with the concept space state
265 disturbance representation (Turner et al. 1993, Fraterrigo & Rusak 2008) but mostly with the
266 tolerance landscape (Rezende et al. 2014), defined by the intensity and duration of a thermal

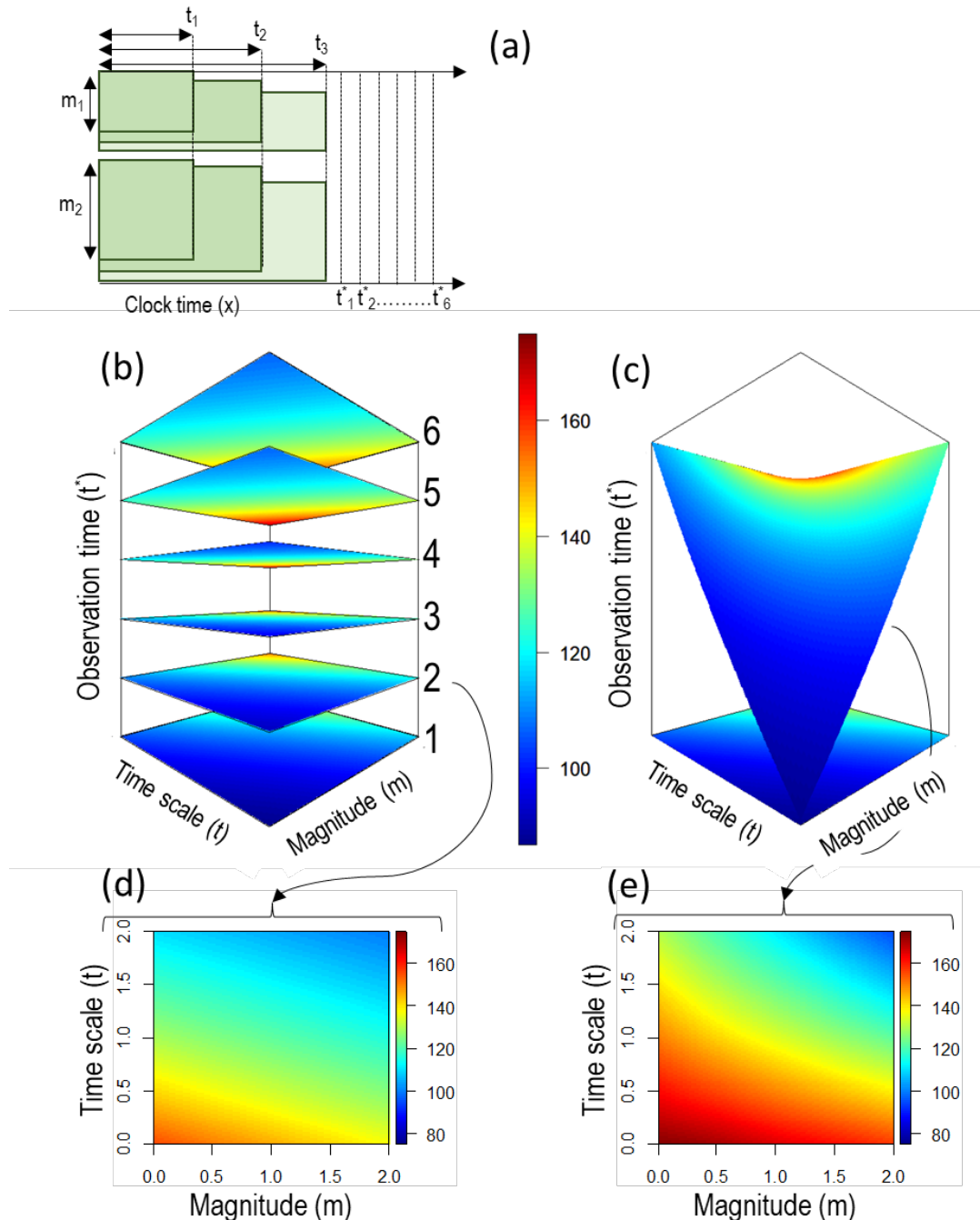
267 stress. This concept may be expanded to a higher number of environmental variables (i.e. not
268 only temperature), with the concomitant increase in the number of dimensions.

269 The second important point is that the metrics used to characterise thermal fluctuation
270 components (e.g. for a heatwave: intensity measured in °C and time in days) is not unique nor
271 absolute. Instead, each point in the space of fluctuations can be located using different
272 coordinate frames. I define the “extrinsic frame” as the one defined by the “observer”, e.g. in
273 clock time and °C. I also define the “intrinsic frame”, as representing how the biological system
274 under study experiences the fluctuations, according to its own traits. For that purpose, I classify
275 biological variables in three types: Type-1: Variables with units of magnitude (e.g. thermal
276 tolerance range) or time (e.g. days to maturation) or driving tolerance and biological time; they
277 give rise to the intrinsic frame. Type-2: Invariant responses: a biological response that occurs
278 within the tolerance range, does not drive tolerance nor biological time and does not have units
279 of time or magnitude. Type-3: Biological rates or sensitivities, i.e. those expressed as per unit
280 of time or tolerance. The role of each variable will be introduced below.

281 As example, I focus on a study of the effect of thermal fluctuations on the body size (the
282 invariant response) of a marine organism (e.g., invertebrate, fish), growing eventually to
283 maturation. For the sake of the example, I assume that body size (the invariant response) does
284 not drive tolerance or biological time. Biological time is the time to maturation; tolerance may
285 be defined in a wide sense, i.e. as the range of preferred temperatures (Gvozdk 2018), based
286 on the aerobic scope (Pörtner 2002), or a range defined from survival or knock-down
287 temperatures (Tang et al. 2000). The same concepts can be applied to other levels of
288 organization: for example, biological time can be quantified for populations (generation time),
289 communities (time scale of change in richness: Ontiveros et al. 2021), and ecosystems (inverse
290 of ratio of production/biomass). Tolerance can also be defined for populations (Gvozdk 2018)
291 and communities (Vinebrooke et al. 2014).

292 In the extrinsic frame (Fig 2), the amplitude ($= m$) is measured in °C and the time scale ($= t$) in
293 clock time, in e.g. days (see Supplement, Section 1, Table S1 for variables and constants). The
294 biological time scale of a fluctuation ($= \tau$) is a unitless quantity, corresponding to the proportion
295 of time from birth to a relevant life history event (e.g., from birth to maturation). The
296 biologically scaled amplitude of the fluctuation ($= \mu$) is defined as a proportion of the thermal
297 tolerance range of the organism, i.e., the capacity of the organism to withstand environmental
298 fluctuations.

299 The next element of the space of fluctuations is the time at which observations are made. In the
300 idealised experiment (Fig. 3a), organisms (originated in the same population) are exposed to
301 fluctuations of different amplitude and time scales. All organisms are kept at the same initial
302 temperature, exposed to the fluctuations, and then returned to the initial temperature before a
303 measurement of body size is taken. The time at which body size is measured is expressed in
304 clock (t^*) and biological scales (τ^*). The observation times considered here (there may be
305 several) occur *after* the fluctuation is experienced (Fig. 3a), i.e. $t^* > t$ and $\tau^* > \tau$. Observations
306 must be done as the fluctuation occurs (see section of worked example), but organisms must
307 experience the full fluctuation before one can causally relate the response to the fluctuation
308 time scale. The time course of the invariant response will occupy the full space of fluctuations,
309 defined by the three axes: amplitude, time scale and observation time (Fig. 3b). Because we
310 assume that temperature drives developmental rates, the time points of observation, at fixed
311 clock time, will not coincide with those at fixed biological times (e.g. at maturation). Therefore,
312 observations at fixed clock vs biological times will lie on different types of surfaces slicing the
313 3D space defined by the fluctuation components and the observation time. The invariant
314 response, observed at fixed clock time lies on flat 2D time slices (Fig. 3b) of the space of
315 fluctuations. By contrast, the response observed at a fixed biological time (e.g. at maturation)
316 will lie on a curved surface (Fig. 3c), with its shape driven by the effect of temperature on the
317 developmental rate (see next paragraph). Consequently, the pattern shown by the biological
318 response will differ between the coordinate frames (Fig. 3c, d).



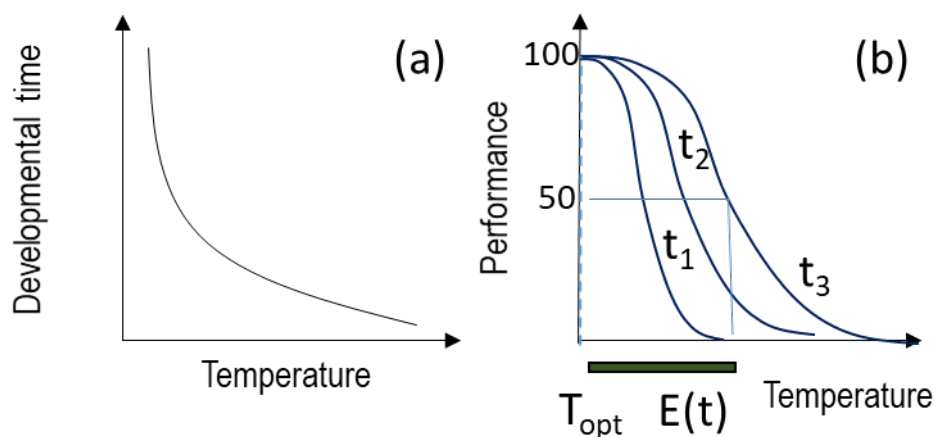
319

320

321 Figure 3. Idealised time course of an experiment quantifying the effect of thermal fluctuations
 322 on the body size (in arbitrary units) of an ectothermic organism at different times, including at
 323 size maturity, with the time of maturation driven by temperature. (a) Diagram of experimental
 324 design depicting a subset of the studied thermal fluctuations as rectangles of different
 325 magnitudes (m_1 , m_2) and time scale (t_1 , t_2 , t_3); clock observation time are given as t_1^* , ..., t_6^* . (b)
 326 At fixed clock time, body size varied through time, occupying the volume defined by m , t and
 327 t^* . Body size, in response to m and t , lies on flat 2D slices (heat map) if observed at fixed clock
 328 times. (c) Body size at maturity however, lies on a curved surface defined by the effect of
 329 temperature on biological time. Panels (d) and (e) illustrate how such an idealised experiment
 330 would show that the effect of thermal fluctuations on body size would depend on the time
 331 coordinate t^* or τ^* .

332 The next step is to define mathematical functions relating the components of the extrinsic frame
 333 (m , t and t^*) with those of the intrinsic one (μ , τ , and τ^*). The functions linking clock with the
 334 biological time scales are given: $\tau(t,m) = t \cdot L$ and $\tau^*(t^*,m) = t^* \cdot L$ where $L(t,m)$ is the
 335 developmental rate, i.e. the inverse of the clock time (=D) required to reach a particular
 336 biological event (e.g. days to maturation). Importantly, $L(t,m)$ is a function of the
 337 environmental fluctuation, not of the observation time (in line with above defined assumptions)
 338 and will be the inverse of the pattern shown by developmental time (Fig. 4a).

339 The biological scaled amplitude of the fluctuation, $\mu(t,m)$, is defined from thermal tolerance
 340 as $\mu = mS$. The function μ (unitless) varies between 0 and any positive value and quantifies
 341 the magnitude of the environmental fluctuation relative to the organismal tolerance range. The
 342 function S is the inverse of the tolerance range (=E, Fig. 1d) which represents how sensitive is
 343 the biological system to the magnitude of the fluctuation. The case $\mu = 1$ corresponds to a
 344 fluctuation that encompasses the full tolerance range, while $\mu \rightarrow 0$ corresponds to situations
 345 where the organism is extremely eurytopic with respect to m ($S \rightarrow 0$ when m is very small with
 346 respect to the tolerance range). I define E with respect to some threshold, for instance the so-
 347 called “knock out temperature” (= M_{out} , i.e., the temperature at which the organism dies or
 348 cease any activity, or it does not respond to stimuli). In synthesis, E is the mathematical
 349 expression of the capacity of the organism to tolerate a fluctuation.



350

351 Figure 4. (a) The curve of developmental time, showing an non-linear decrease with
 352 temperature; this curve is modelled subsequently in Eqs. (4) & (5) in Results. Developmental
 353 time depends only on the amplitude of the thermal fluctuation $D = D(m)$ as in the case of
 354 phenology models based on degree days, but such assumption does not restrict the analysis.
 355 (b)The tolerance range is defined for different fluctuations time scales (t_1, t_2, t_3), used to obtain
 356 the term S , included subsequently in Eqs. (3) & (6) in Results.

3.2 Invariant responses

The invariant biological response (body size, Fig. 3b) is a type of response that does not drive tolerance and it is not a rate of change with respect to any of the coordinate frames. The invariant response exists within the limits stated by the biological time and tolerance, i.e. there is a “region of existence”, within the space of fluctuations. This response is represented by a continuous and differentiable function and the invariance property results in that:

$$R(t, t^*, m) = r(\tau, \tau^*, \mu) \quad (1)$$

The invariance property is the reason why rates are not considered at this stage. Rates are partial derivatives of the invariant response (see below) and their magnitude depend on the coordinate frame. The differentiability assumption enables to represent the effect of the thermal fluctuation on the response through partial derivatives with respect to the amplitude and period; the same idea applies to a general environmental fluctuation characterised by two or more quantitative descriptors. Hence, I define the effect of each variable of the invariant response as system of partial differential equations (PDE, Giménez et al. 2022), which in matrix formulation gives:

$$\begin{bmatrix} \frac{dR}{dm} \\ \frac{dR}{dt} \\ \frac{dR}{dt^*} \end{bmatrix} = \begin{bmatrix} \frac{d\mu}{dm} & \frac{d\tau}{dm} & \frac{d\tau^*}{dm} \\ \frac{d\mu}{dt} & \frac{d\tau}{dt} & \frac{d\tau^*}{dt} \\ \frac{d\mu}{dt^*} & \frac{d\tau}{dt^*} & \frac{d\tau^*}{dt^*} \end{bmatrix} \cdot \begin{bmatrix} \frac{dr}{d\mu} \\ \frac{dr}{d\tau} \\ \frac{dr}{d\tau^*} \end{bmatrix} \quad (2)$$

In a more compact notation, equation (2) may be written as $\mathbf{R} = \mathbf{M}\mathbf{r}$ where \mathbf{R} and \mathbf{r} are vectors of derivatives of R and r respectively; both \mathbf{R} and \mathbf{r} contain biological rates and sensitivities with respect to magnitudes and time scales. The matrix \mathbf{M} transforms the rates of the intrinsic to the extrinsic frame; the inverse of \mathbf{M} will do the reverse transformation. In equation 2, the third entry of the second row of \mathbf{M} (in bold) is set to zero, when the observation time varies independently of the time scale of the fluctuation (fixed clock observation time). In practice, t^* is constrained to be longer than the longest fluctuation time scale used in an experiment; however, within such limits, one can observe the response at any desired time. In addition, the first two entries of the last row of \mathbf{M} (in bold) are set to zero because the observation time, (t^* , τ^*) does not affect the biological tolerance (μ) nor the biological time scale of the fluctuation (τ). This follows from the fact that we ignore (for simplicity) the timing of the fluctuation as a component. In a more general case, such timing would be an additional component giving an extra dimension to the space of fluctuations.

386 Working with the response and the mapping functions is facilitated by two properties: (1) They
387 should approximate to continuous and differentiable functions, so that the terms in M and the
388 derivatives of R exist. Modelling of tolerance is sometimes carried out through conditional
389 functions but the alternative is to fit appropriate smooth functions to overcome the problem.
390 (2) Mapping functions should be bijective (i.e. always increasing or decreasing), so as to
391 provide a one-to-one, mapping. Such functions ensure the existence of direct and inverse maps,
392 from each point of the extrinsic to each point of the intrinsic frame. Not all functions of
393 developmental time are like this; instead, some show a minimum at an extreme high
394 temperature threshold, followed by a maximum (Shi et al. 2016). Issues associated to (1) and
395 (2) can be solved in practice by modelling different parts of the space of fluctuations as separate
396 regions.

397 **3.3 Scenarios of analysis**

398 There are several scenarios for how the tolerance range and biological time drive the effect of
399 the fluctuation on the invariant response. (1) The trivial scenario where neither E nor L are
400 affected by the fluctuation traits. Both the extrinsic and intrinsic frames coincide and the effect
401 of the fluctuation on the body mass does not change with the coordinate frame. (2) Where E is
402 not affected by the fluctuation traits: in such a case (discussed in Giménez et al. 2022), μ is
403 proportional to m . (3) The scenario explored here, where both E and L depend on some property
404 of the fluctuation being experienced.

405 The nature of the intrinsic frame depends on how biological time and tolerance are shaped by
406 the fluctuations. I consider three cases: in Cases 1 and 2 increased temperatures would result
407 in a deleterious effect on performance (Niehaus et al. 2012). Case 1 is based on simple functions
408 that help to visualise and obtain qualitative understanding of the differences between the
409 extrinsic and intrinsic frames. Case 1 is related to Case 2, which introduces empirical functions
410 and enables a realistic view of chronic negative effects of fluctuations. Case 3 introduces
411 adaptive plasticity by which the fluctuation has positive effects on the tolerance range. While
412 in cases 1 and 2, I simulate the response observed at a fixed clock time, in case 3, I simulated
413 the time course of the response.

414

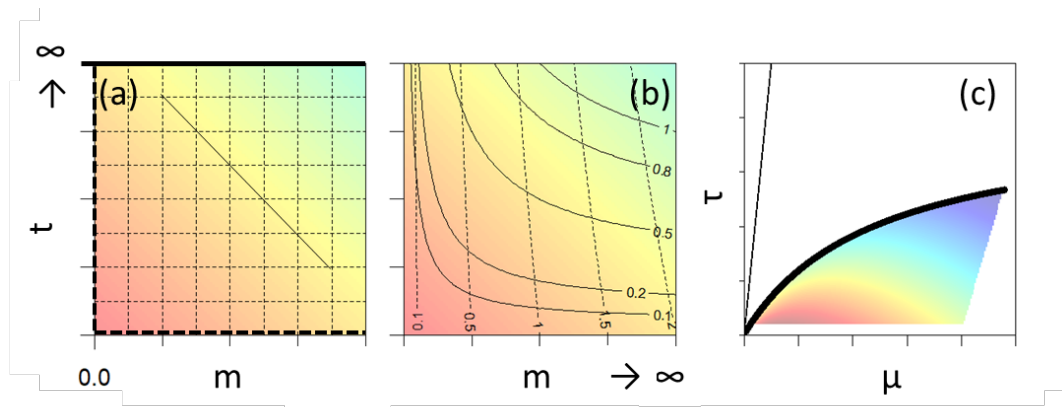
415

416

417

4. RESULTS

418 The central point in SOFiA is that the space of fluctuations is represented using different
 419 coordinate frames, related through non-linear functions. It is important to clarify the two
 420 different types of representations: First, one can represent a time slice defined either at a fixed
 421 clock time or at a fixed biological time (see Fig. 3b, c). Second, for each time slice one can
 422 represent two projections, based respectively on the extrinsic (mt-projection) or intrinsic
 423 coordinates ($\mu\tau$ -projection). For cases 1-3, I focus on time slices at fixed clock time (fixed t^*):
 424 this represents the simplest possible experiment and enables better understanding of the
 425 different projections; the slice at a fixed biological time is explored in the worked example.
 426 Given a (fixed) time slice, fluctuations are plotted in the upper half of a plane (Fig. 5a, details
 427 in Supplement Section 2), where $t > 0$ (fluctuations of negative time scale do not exist). In
 428 addition, none of the fluctuations will occur at $m = 0$ or $t = 0$ because such fluctuations do not
 429 exist either. For simplicity, I will assume that $m > 0$ because experiments usually focus on
 430 either high or low temperature with respect to a thermal optimum, for which m can be
 431 conveniently rescaled to be positive. Hence, the fluctuations of interests are plotted in the first
 432 quadrant (Fig. 5a) and the properties mentioned below do no change if m is negative.



433

434 Figure 5. A time slice of the space of fluctuations at fixed clock time, showing a biological
 435 response $R = 100-t-m$ as a heat map. (a) mt -projection with mt -isolines given by straight lines
 436 (i.e. as a cartesian frame). In the heatmap of R , isolines (lines of indicating equal R -values) are
 437 given by diagonals (note colour gradient) and one such diagonal is shown as a continuous line.
 438 The horizontal top line represents the line at infinity corresponding to constant conditions.
 439 Dashed lines at $m = 0$ and $t = 0$ are open boundaries. (b) mt -projection with $\mu\tau$ -isolines given
 440 by curves, (here taken from Case 1), with all parameters of Eq. (3) & (4) set to = 1, except
 441 $k_\mu = 0.1$. (c) $\mu\tau$ -projection. The space occupied by the fluctuations is constrained to the coloured
 442 area by the maximum values of m and t ; these represent the maxima used in a realistic
 443 experiment. The thick black curve is the upper limit set by the maximum value of t and the
 444 straight line is the theoretical maximum. Isolines of equal body size (diagonals in a-b) form
 445 petal-like curves in (c) and the parabolas of (b) would give straight lines in (c).

446 **4.1 Case 1: hyperbolic model**

447 For tolerance, I use an inverse function $E = E(t) = 1/(S_0+k_\mu t)$, with $S(t) = (S_0 + k_\mu t)$. Here, S
448 increases linearly with the time scale of the fluctuation, from a minimum S_0 defined as $1/T_{max}$;
449 the constant k_μ is a rate of increase. In such a case we obtain:

450
$$\mu = m(S_0 + k_\mu t) \quad (3)$$

451 In addition, I will assume that developmental time follows an inverse function of temperature,
452 such that:

453
$$\tau = t(D_{min} + k_\tau/m)^{-1} \quad (4)$$

454 where D_{min} is the asymptotic minimum developmental time achieved, as $m \rightarrow \infty$, in the absence
455 of developmental impairments.

456 The values of the intrinsic frame define a non-linear and non-orthogonal coordinate frame (Fig.
457 5b). Equations 3 and 4 define hyperbolic curves, as lines of equal τ (or μ) in a similar way as
458 the straight lines in define lines of constant m or t (Fig. 5a). Consecutive lines define areas of
459 different size with the shape of such area depending on the constants (S_0 , D_{min} , k_μ , k_τ) driving
460 the tolerance and developmental time. Such lines do not meet at straight angles reflecting the
461 fact that μ and τ are not mutually independent variables.

462 An alternative view of the response, highlighting the organismal perspective, is given by the
463 “ $\mu\tau$ -projection” (Fig. 5c). This is analogous to the projection obtained from principal
464 component analysis, where communities are represented as points in a space. Before the PCA
465 is carried out, the original projection (analogue to the mt-projection here) would have species
466 abundances as axes. The difference is that the PCA-axes are linear and orthogonal, while $\mu\tau$ -
467 axes, are curvilinear and non-orthogonal. Consequently, in the $\mu\tau$ -projection, the fluctuations
468 are constrained to a triangular region characterised by open boundaries (coloured area in Fig
469 5c) and with the region being set by logistical and theoretical limits (see Supplement: Section
470 2).

471 Provided with the projections defined above, and focusing on the perspective of the organism,
472 I highlight the following points:

- 473 1. Space of existence: The region where $\mu \leq 1$ and $\tau \leq 1$ defines the “space of existence”,
474 i.e. where the response R exist. This is because $\mu > 1$ implies that the temperature is
475 higher than the tolerance range (hence the organism collapses). In addition, $\tau > 1$

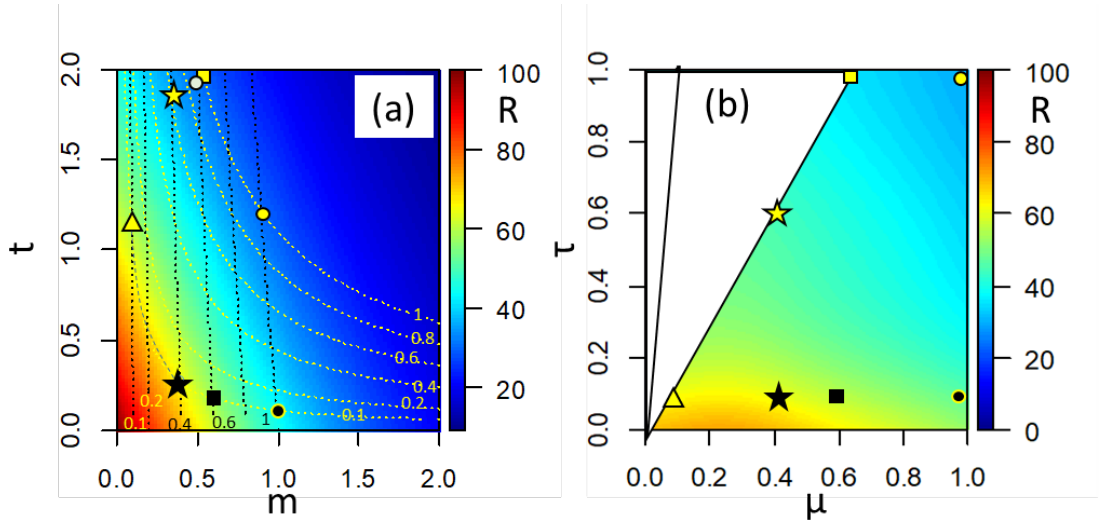
476 implies that the time scale of the fluctuation is longer than the time to maturation;
477 therefore, one cannot establish a causal relationship between biological time and the
478 fluctuation time scale. In other examples, the space of existence will be set at $\tau \neq 1$ (see
479 “Discussion”).

480 2. Extreme event and biological definition of heatwave: extreme events (i.e. a fluctuation
481 compromising organismal existence) are represented by the set of fluctuations defined
482 by the curve $\mu=1$. Notice that such curve defines fluctuations differing in amplitude
483 and clock time scale. If extreme events are used as a biological definition of heatwave,
484 then such definition would differ from that based on climatology. For instance, marine
485 heatwaves are defined as those thermal fluctuations where the temperature exceeds a
486 fixed threshold (the 90th percentile of a temperature distribution), for 5 or more days
487 (Hobday et al. 2016). By contrast, the definition arising from the μ -curves does not use
488 fixed temperature and time scales.

489 3. From the standpoint of the organisms, differences among fluctuations are defined by
490 the values of μ and τ (not m and t). From the extrinsic perspective, straight lines (i.e.
491 the Euclidean distance) should define the difference (=shortest distance) between any
492 two fluctuations (Fig. 5a; also recall the analogy to PCA for ecological communities).
493 However, from the intrinsic perspective, the shortest distance between any two
494 fluctuations is given by the hyperbolic curves (Fig. 5b). Hence, whether two
495 fluctuations are experienced by the organism as very different or rather similar depends
496 on the distance along the hyperbolic curves. In this case, the projection in the $\mu\tau$ -plane
497 (Fig. 5c) might give a more intuitive view of the differences among fluctuations, from
498 the organismal perspective.

499 4. The invariant response (body size at maturation) is distorted as we compare the different
500 projections (Fig. 6). The distortion reflects important biological effects of temperature
501 on both tolerance and biological time. In the simulation (details in Supplement: Section
502 3), the invariant response is more sensitive to m than to t (equation in Fig. 6) but it
503 becomes more sensitive to τ than to μ (compare change in colour gradient in Fig. 6a vs
504 Fig 6b). The distortion reflects the fact that the organism will experience the response
505 as being different from what is shown by the extrinsic frame.

506 Next, Case 2 uses realistic functions and highlights (by comparison to case 1) properties that
507 are robust to changes in the mapping functions.



508

509 Figure 6. A time slice of the space of fluctuations at fixed clock time (a) mt -projection with
 510 intrinsic coordinate frame included: (b) $\mu\tau$ -projection. Different symbols in (a) represent
 511 fluctuations which are shown in (b) to highlight the deformation produced by the intrinsic
 512 frame. The diagrams were constructed within the range (0, 2) for both t and m . The mapping
 513 functions are as follows: Eq. (3): $S_0 = 1$, $k_\mu = 0.1$, Eq. (4): $D_{min} = 1$, $k_\tau = 1$. The response was
 514 modelled as $R = 100 \cdot \exp(-0.4m - 0.8t)$.

515

516 4.2 Case 2: Combining metabolic theory and thermal tolerance

517 Here, I consider empirically obtained functions for developmental time and tolerance and use
 518 mt -projection to focus on the region of existence and on the definition of extreme events.
 519 Developmental time is defined in the metabolic theory of ecology of Brown (2004), such that:

520
$$\tau = tL_{max} \cdot e^{\frac{-A}{(m+273)}} \quad (5),$$

521 where m is the temperature (in $^{\circ}\text{C}$), L_{max} is the inverse of the asymptotic minimum of
 522 developmental time and A is the ratio of activation energy (0.64 eV) and the Boltzmann
 523 constant ($8.617 \cdot 10^{-5} \text{ eV Kelvin}^{-1}$).

524 The effect of the fluctuation is modelled following work on thermal death times (Bigelow 1921,
 525 Urban 1994, Tang et al. 2000, Rezende et al. 2014, Jorgensen et al. 2019). Those studies show
 526 that responses to temperature can be modelled with two separate functions: (1) A thermal range
 527 characterised by moderately high (or low) temperatures, where survival is independent of the
 528 exposure time. Responses in this range are equivalent to those covered in Giménez et al. (2022)
 529 where μ is proportional to m , because E would not vary with time. (2) Beyond a thermal
 530 threshold, E decreases linearly with the logarithm of exposure time. I focus on this range,
 531 assuming that the tolerance range is proportional to the logarithm of the time scale of the

532 fluctuation. Here, $E(t)$ depends on the knockout temperature ($= M_{out}$) according to the equation
 533 $M_{out} = M_{crit} - z\varepsilon_1 \log(t\varepsilon_2)$. Here, M_{crit} is the knockout temperature corresponding to a unit of
 534 clock time ($t = 1$), z is the sensitivity of M_{out} to change in $\log(t)$. In addition, ε_1 and ε_2 are
 535 proportionality constants ($= 1$) and are no longer considered. By setting $E_{max} = M_u - M_{crit}$
 536 (maximum tolerance range), we obtain: $E(t) = E_{max} - z\log(t)$. In such a case the biological
 537 magnitude in the intrinsic frame (μ) is given by the equation.

$$538 \quad \mu = \frac{m}{[E_{max} - z \cdot \log(t)]} \quad (6)$$

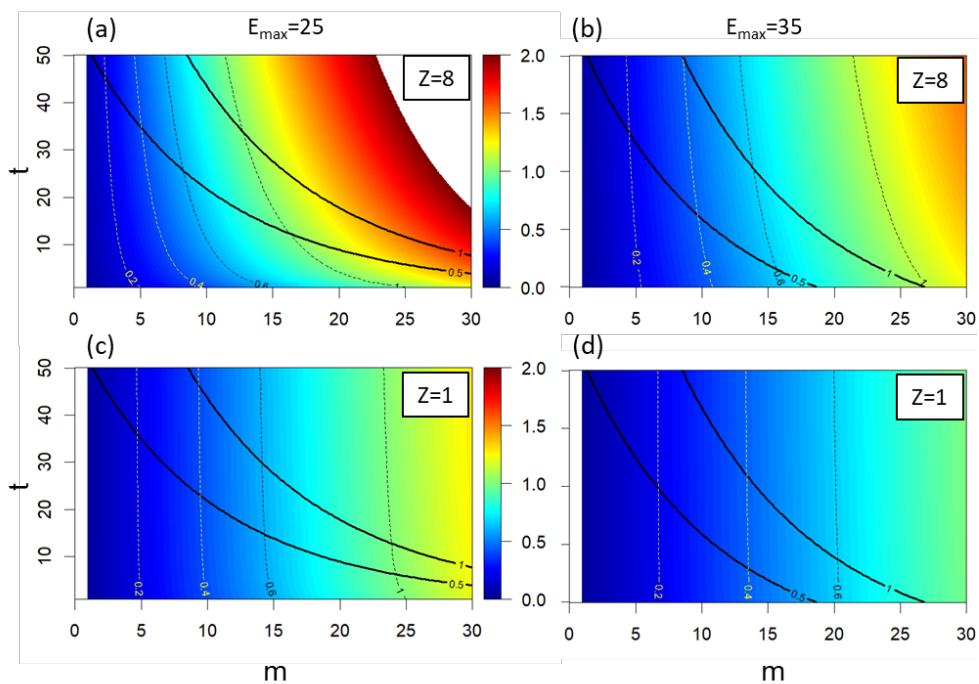
539 As in Case 1, the lines at $\mu = 0$ and $\tau = 0$ are open boundaries, and the lines of constant μ or τ
 540 are curves, representing a non-orthogonal reference frame that will also deform any invariant
 541 response (further similarities discussed in Supplement: section 4). In the mt-projection, values
 542 of μ (heat maps in Fig. 7), capture the general pattern observed by studying thermal death times
 543 i.e., low amplitude but long period fluctuations can be as bad as high amplitude short period
 544 ones.

545 Case 2, based on empirical models, gives again a definition of extreme event as in Case 1,
 546 where the critical temperature defining the heatwave (here represented as m) depends on the
 547 clock time scale of the thermal fluctuation (Fig. 7); here, the position of the curve $\mu = 1$ depends
 548 on $\log(t)$. In addition, the set of extreme fluctuations and the region of existence depends on
 549 the thermal sensitivity (z) and the maximum tolerance range (E_{max}). At high z and narrow E_{max}
 550 (Fig. 7a), the region of existence is constrained to fluctuations that are shorter than the time to
 551 maturation ($\tau = 1$). In the simulation, there is only a narrow region ($t > 30$ in Fig. 7a) where
 552 the curve of the extreme fluctuations ($\mu = 1$) is located to the right of the curve of $\tau = 1$. This
 553 indicates that extreme fluctuations occur at time scales longer than the time to maturation. At
 554 other combinations (Fig. 7b-d) such region expands; for instance, for $z = 1$ and $E_{max} = 35$, most
 555 of the extreme fluctuations occur at time scales that are longer than time to maturation (Fig.
 556 7d).

557 It is important to note that the interpretation of the isolines $\mu = 1$ and $\tau = 1$ depends on the
 558 specific case. For example, it may not be possible to quantify tolerance beyond maturation, i.e.
 559 in the region located to the right where $\tau > 1$ (the maximum time scale covered in the
 560 experiment). Likewise, in the region where $\mu > 1$, developmental time cannot be quantified.
 561 However, tolerance may be quantified in the region where $\tau > 1$ in the case of e.g., a
 562 multigenerational study where the biological time is defined as generation time. In an example
 563 of organisms growing to metamorphosis (instead of maturation), scenarios where the curve μ

564 = l is located to the right of $\tau = l$ would indicate that reaching a critical life history stage (e.g.
 565 metamorphosis) has the potential to “rescue” the organism (or population) from the
 566 consequences of an extreme fluctuation. For species experiencing metamorphosis and habitat
 567 shifts, thermal conditions before the shift may not be the same as in the post-shift habitat.
 568 Alternatively, organisms may experience shifts in capacity to tolerate increased temperatures,
 569 for instance in association to a metamorphosis: larval stages are usually more sensitive than
 570 juveniles and adults (Pandori & Sorte 2019). In both cases, reaching metamorphosis would be
 571 analogous to reaching a thermal refuge. In semelparous species, reaching maturation and
 572 reproduction ($\tau = l$) is central, but post-reproductive life ($\tau > l$) is of no relevance for fitness.
 573 In any case, SOFiA captures important aspects of ontogeny, physiology, and phenology as
 574 drivers of responses to extreme events.

575



576

577 Figure 7. Case 2: A time slice of the space of fluctuations at fixed clock time showing a heatmap
 578 of μ based on equation 6. Each panel has different values of z and E_{max} (i.e. tolerance range at
 579 $t = l$). Dashed lines are selected lines of constant μ : note that at small z , μ becomes proportional
 580 to m and less dependent on t . Continuous lines are lines of constant τ (Eq. 6, $L_{max} = e^{22.47}$).

581

582

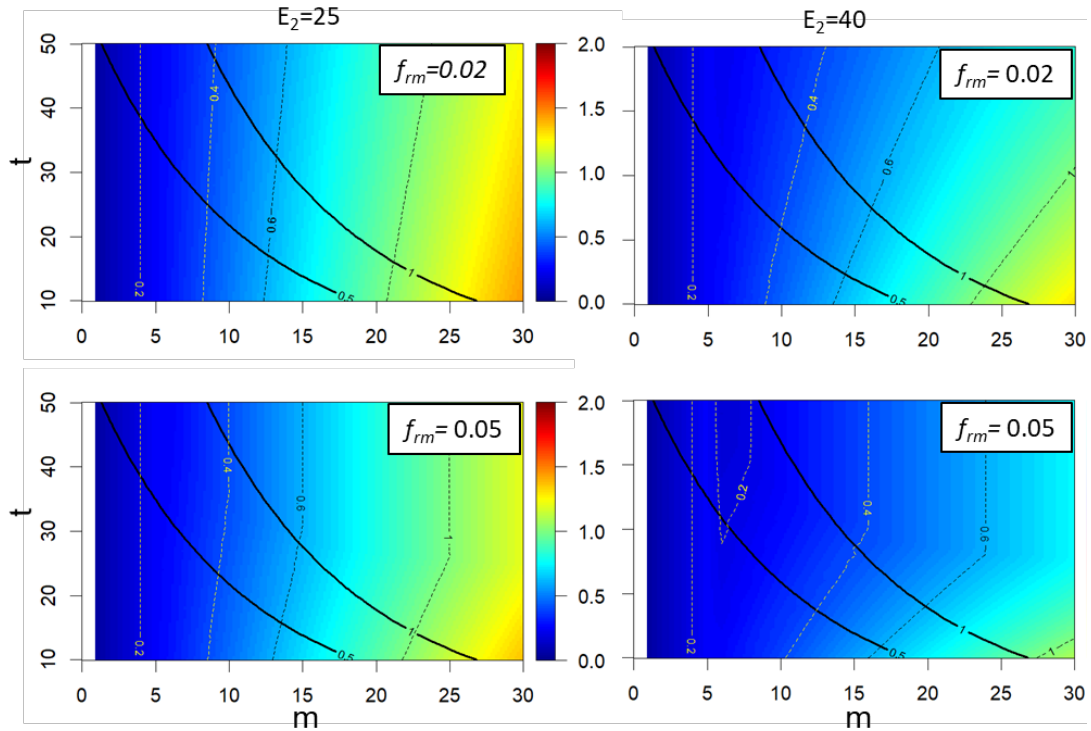
583

584 4.3 Case 3: Role of adaptive plasticity

585 In the above cases, the tolerance depended only on the time scale of the fluctuation. However,
586 the presence of adaptive plasticity should (within limits: DeWitt et al. 1998) either shift or
587 expand the tolerance range (Angiletta 2009, chap. 5; Seebacher et al. 2014, Salachan et al.
588 2022) in response to the (thermal) fluctuation. We can visualize the rescue effect of adaptive
589 plasticity as an expansion of the space of existence in the mt -representation (see below).

590 Plasticity involves three main steps (Windig et al. 2004); i.e. where (1) a cue is converted to a
591 signal (e.g. hormones: Duffy et al. 2002) that (2) triggers a change in the phenotype which
592 results in (3) a change in its performance (= tolerance). Those steps lead to a latency period
593 (Laubach et al. 2022) between the moment when an environmental cue is detected and when
594 the phenotype is functional. The latency period varies according to the type of plasticity: from
595 short (hardening: Hoffmann et al. 2003), through developmental (Salachan and Sorensen 2017)
596 to transgenerational plasticity (Donelson et al. 2012). The relationship between the latency
597 period and the time scale of the fluctuation may range between two extremes. On one extreme,
598 the fluctuation may be perceived as a short-term pulse with respect to such period (Manenti et
599 al. 2018) while on the opposite extreme the fluctuation is perceived as a long period wave. In
600 the first case, the tolerance range depends on whether the organisms (or the parents)
601 experienced a previous fluctuation. In such a case, we may define the acclimation state of an
602 organisms as $E_i(t)$ which will shift from $E_1(t)$ to $E_2(t)$ after a fluctuation is experienced. One
603 may model such change of state as a change in the parameters defining the equations of case 2
604 (previous section).

605 I focus on the case (Fig. 8) where the latency period can be much shorter than t so that (1) the
606 acclimation state changes as the fluctuation is experienced and (2) the fluctuation can be
607 sufficiently long to alter developmental time. An example is the acclimation to seasonal
608 fluctuations in temperature where organisms acclimate to summer (or winter) conditions well
609 in advance of the time of maximum (or minimum) temperatures. I model those steps through
610 functional responses, with the overall result that changes in the cue (temperature) are mapped
611 into changes in the thermal tolerance and μ (Fig 8). This simulation differs from cases 1 and 2
612 in that here I modelled the time course of the response (details in Supplement: section 5). I do
613 not intend to develop a mechanistic model (see e.g. Hazel et al. 1990, Buoro et al 2012) and I
614 must emphasise that the model is intended as illustration of how plasticity can be incorporated
615 to SOFiA.



616

617 Figure 8. Case 3, Adaptive plasticity: A time slice of the space of fluctuations at fixed clock
 618 time showing a heatmap of μ . Different panels (a-d) show μ for different values of maximum
 619 tolerance range ($E_2 = 25$ and $E_2 = 40$) expanded from a value of $E_2 = 20$ before the fluctuation
 620 is experienced. The inset values correspond to the maximum rate of phenotypic change ($=f_{rm}$)
 621 as driven by temperature (equations in Supplement, Section 5). In all panels, the signal
 622 activation threshold was at 5°C : this is best noted at $E_2 = 40$ and $r_{max} = 0.05$. Continuous lines:
 623 constant τ -values; dashed lines: constant μ -values.

624

625 The rescue effect of adaptive plasticity is shown as the expansion of the region of existence:
 626 the curve $\mu = 1$ is shifted to the right (as compared to Cases 1 and 2). Hence, the rescue effect
 627 is manifested in the set of fluctuations defining extreme events. As compared to the previous
 628 cases, extreme events occur at high values of m . The region where the plastic response operates
 629 depends on the three main steps: (1) The threshold response to the cue: below some thermal
 630 threshold (fixed to 5°C in Fig. 8 and 10°C in the supplement, Fig. S4) the plastic response is
 631 not triggered ($m < 5^\circ\text{C}$ in Fig. 8). The tolerance range is still wide (giving low μ values). In the
 632 model, the threshold response is driven by the thermal threshold y_u of the first functional
 633 response:

634

$$F_{c \rightarrow s} = \frac{1}{1 + e^{k_s[y_u - y(x)]}} \quad (7)$$

635 where $F_{C \rightarrow S}$ is the function converting a cue to a signal, $y(x)$ is the temperature fluctuating
636 through clock time ($=x$) and k_S is a rate constant indicating how sharp is the triggering of the
637 response.

638 (2) The rate of phenotypic change in response to temperature f_r :

639
$$f_r = \frac{f_{rm} \cdot y}{k_r + y} \quad (8),$$

640 where f_{rm} is the maximum rate of phenotypic change and k_r is the half saturation constant in
641 the model; the inverse of f_{rm} is time scale, defined here as the minimum latency period.

642 This rate is the component of the second functional response:

643
$$F_{S \rightarrow P} = f_{sp1} + \sum_x f_r(x) \quad (9)$$

644 $F_{S \rightarrow P}$ maps the signal to the phenotypic state (as a continuous variable) from an initial state, f_{sp1}
645 (before the signal activates the response) up to an upper threshold $= f_{sp2}$, remaining constant
646 thereafter. Because Eq. (9) has an asymptotic maximum (f_{rm}), the rate of phenotypic change is
647 constrained; in consequence, if the time scale of the fluctuation is sufficiently short, there is no
648 sufficient time for the plastic response to reach its maximum value. Hence, plasticity operates
649 on the μ values at intermediate values or m an t (at moderately high m).

650 (3) The maximum thermal tolerance range, defined in the third functional response of the
651 model, $F_{C \rightarrow S}$, which maps the phenotype to the thermal tolerance. This function is linear
652 between the lower ($= E_1$) and the upper tolerance range ($= E_2$) and defines the region of
653 existence in Figure 8.

654 **4.4 Worked example**

655 The worked example (Fig. 9, details in Supplement: Section 6, and data files) represents an
656 experiment aimed at (1) quantifying the effect of the magnitude and time scale of thermal
657 fluctuations on the body size of a marine ectotherm and (2) estimating the average body mass,
658 given a set of fluctuations of varying magnitude and time scale. The example represents
659 experiments taking place over several weeks to few months, which corresponds to those carried
660 out with short lived organisms (e.g. copepods) or a specific life phase of a long lived species
661 (e.g. larvae). Biological time is referred up to maturation (copepods) or metamorphosis (fish
662 or invertebrate larvae). In both cases, temperature has a strong effect of developmental time
663 (copepods: Guerrero et al. 1994, McLaren 1995; marine larvae: O'Connor et al. 2007); hence,
664 the functions mapping the time coordinates are important. For example, within species

665 increased temperature can reduce larval developmental time by 50% over the tolerance range,
666 which can span 10-15°C (but varies among species: O'Connor et al. 2007). Increases of only
667 3°C can have important reductions in developmental time towards the lower sector of the
668 thermal tolerance range: for example, in one of the best studied crustaceans, the shore crab
669 *Carcinus maenas* an increase in temperature of 3°C reduces the larval developmental time (to
670 megalopa or first crab stage) by a 25 to 35% within the range 12-18°C, corresponding to
671 summer temperatures in the distribution range (Dawirs 1985, DeRivera 2007, Šargač et al.
672 2022). The functions mapping time coordinates become more important at that sector,
673 especially under long fluctuation time scales. At the upper sector of the thermal tolerance range,
674 biological time is little affected by temperature; however, at that sector, the functions mapping
675 from the extrinsic to intrinsic magnitude coordinates should become important if tolerance
676 depends on the time scale of the fluctuation.

677 The experiment follows a gradient design (Kreyling et al. 2018) with 10 levels of thermal
678 magnitude crossed with 9 levels of time scales, giving 90 locations (i.e. combinations of time
679 scales and magnitudes) in the space of fluctuations. Organisms are observed every day in order
680 to record the time at maturation and the time at which they reach the thermal limit (i.e. they die
681 or exhibit a predefined behavioral response). In the first step, non-linear regression models are
682 used to obtain the equations giving the τ , μ , size after 70 days of experiment, $R_1(m, t, t^* = 70$
683 $days)$, and size at maturation $R_2(m, t, \tau^* = 1)$. For the second objective, the functions R_1 and R_2
684 are used to estimate the average response through scale transition theory, model simulations
685 and the so-called mean field approach.

686 The constraint on the number of times at which size can be observed reproduces a realistic
687 experiment where animals die beyond the region of existence and where measurements of body
688 size is too invasive to be performed more than twice or where there are logistical constraints.
689 With some caveats (see next paragraph) the example may also be taken as a case study of a
690 species monoculture (e.g. macroalgal or mussel bed) or natural community, recovering after a
691 disturbance event, where the biological variables are generation time (or the inverse of species
692 replacement rate), tolerance (or species richness) and biomass (or some ecosystem service).

693 In the worked example, the curves $\mu = 1$ and $\tau = 1$ cross each other as expected if some of the
694 fluctuations enable maturation, but others kill organisms before reaching maturity. In other
695 situations, such curves may not cross, but the experiment will still provide valuable
696 information. If all animals reach maturity, the experiment will quantify the dependence on body

697 size on the time coordinate frame. If by contrast, thermal thresholds are reached before
698 maturation, the experiment would provide information about the region of existence and
699 identify the set of fluctuations defined as extreme (i.e. the set defined by the curve $\mu = 1$).

700 The importance of the mapping function is given by the following points. First, the function
701 $\tau^*(m, t, t^*)$, mapping coordinates of observation time, shows that responses differ considerably
702 depending on whether we quantify size at maturation or at a given clock time. The difference
703 is shown in maps of figure 9 (contrast Figs. 9a-b vs 9c) and in the estimated body size given
704 an average heatwave (Table 1: compare R_1 vs R_2). Second, the function $\mu(m, t)$, quantifies the
705 effect of the time scale of the fluctuation on thermal tolerance; it predicts which heatwaves
706 would result in system collapse: this is illustrated in Figure 9b as the white area, which
707 corresponds to heatwaves with combinations of magnitudes and time scales (m and t
708 coordinates) leading $\mu(m, t)$. Third, the combination of the above-mentioned functions predicts
709 the set of heatwaves still enabling animals to be “rescued” by achieving maturity (or
710 metamorphosis): this is illustrated in Figure 9b as the portion of the curve $\tau^* = 1$ lying at the left
711 of the curve $\mu = 1$ (i.e. not in the white area). Fourth, the combination of $\mu(m, t)$ and $\tau(m, t)$
712 predicts the set of fluctuations of a time scale equal than the time to maturation (or to
713 metamorphosis) are not tolerated. This is illustrated in Figure 9b the curve $\tau = 1$ (dashed line)
714 lying at the right of the curve $\mu = 1$, if $m > 5$; the portion lying at the left of the curve $\mu = 1$ is
715 predicted to occur if larvae experience fluctuations of time scales larger than 50 days.

716 In interpreting R_1 and R_2 (Figs 9b, c) one must recall that such functions are on different
717 surfaces that cut the volume representing the time course of the invariant response (Fig 3). The
718 difference between R_1 and R_2 (Fig. 9b, c) is carried out by the modelling of the average response
719 (Table 1) to a set of fluctuations (Fig. 9c), but in both R_1 and R_2 , the mean field approach
720 underestimates the average response as compared to simulating from the model or applying
721 scale transition theory.

722

723

724

725

726

727

728

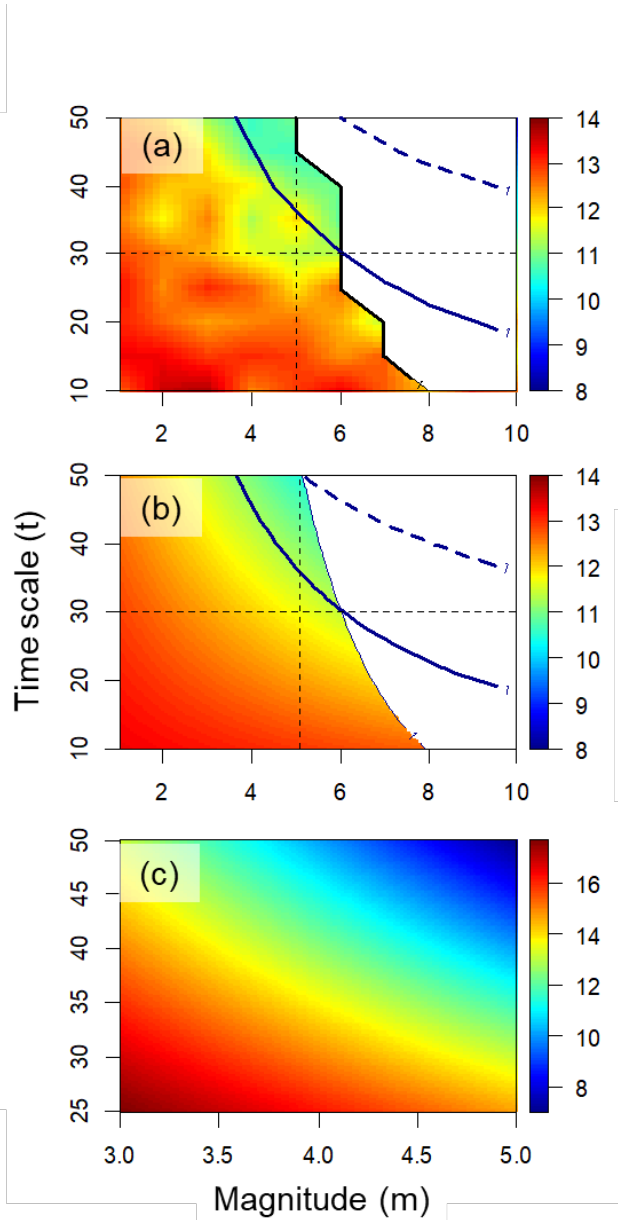


Figure 9. Worked example. Simulation of an experiment quantifying the role of magnitude and time scale of thermal fluctuations on body size (color heatmap) of a marine organism at maturation. (a) mt-projection of the observed response at a fixed clock time ($t^* = 70$ days). (b) Fitted curves and body size at the same fixed clock time as in (a). (c) mt-projection of the fitted response at maturation. The projections in (a) and (b), correspond to a flat time slice (see Fig 3): the $\mu = 1$ curve is the black line delimiting the white area (i.e. no data at $\mu > 1$). The curve of the time at maturation, $\tau^* = 1$, is given as a continuous blue line; the dashed blue line corresponds to the curve of $\tau = 1$ (fluctuation with time scales of the maturation time). The curves of τ^* and τ differ because they are scaled to different time variables. The vertical dashed line delimits the region (to the left) where maturation is reached irrespective of the time scale of the fluctuation. The horizontal dashed line delimits an upper region where maturation can be reached. The heatmap in (c) lies on a curved surface (see Fig. 3) and it is restricted to the region of the space of fluctuations enabling maturation (note axis ranges). The data (csv file) and procedures are given in Supplement, Section 6.

761 Table 1. Estimated body size (in arbitrary units) at $t^* = 70$ days
 762 (R_1) and at maturation (R_2) based on mean field approach, scale transition theory and model
 763 simulation.

	R_1	R_2
Mean field	11.95	14.12
Scale transition	11.92	14.03
Simulation	11.92	14.03

764

765

766

767

5. DISCUSSION

768 Here, I presented a geometric approach (SOFiA) to understand biological responses to
769 temperature (or other environmental fluctuations), from the perspective of organisms. This
770 approach expresses the organismal perspective as a coordinate frame within a space defined by
771 fluctuation components and the times at which observations are made in an experiment. Using
772 temperature as example, I showed how this approach ingrates our current knowledge about
773 effects of environmental variables on organisms. We know that temperature has strong non-
774 linear effect on biological time (McLaren 1995, Gillooly et al. 2001); that thermal tolerance
775 decreases non-linearly with the exposure time (Rezende et al. 2014), and that adaptive plasticity
776 has a characteristic time course (Windig et al. 2004). The organismal perspective is obtained
777 from the relationship between different types of biological traits: (1) traits driving tolerance
778 and biological time provide the metric for the biological scaled magnitude and time of a
779 fluctuation. (2) There are traits, called invariant responses, responding to tolerance and
780 biological time. (3) Traits defined by rates are identified as those with magnitude depending
781 on the reference frame. In addition, the geometric approach presented here highlights the
782 importance of considering the frame used to scale the time at which observation are made
783 because of its consequences in the observed invariant response. The result is the capacity to
784 quantify biological responses in different frames which should lead to better mechanistic
785 understanding; in addition, the approach presented here is able to provide predictions for field
786 conditions (through e.g. scale transition theory: as shown in the worked example).

787 A main feature of SOFiA is the mathematical formalism, represented by a set of functions and
788 partial differential equations. One may argue that this is merely a formalizing exercise only
789 providing more precision. However, the mathematical formalism is central to identify counter-
790 intuitive results arising from interactive effects and non-linearities. A similar approach has
791 helped to identify the conditions where interactive effects, occurring at a level of organization
792 (e.g. individuals), are not mapped into a higher level of organization (population: DeLaender
793 2018). Likewise, the mathematics of scale transition theory (Denny & Benedetti-Cecchi 2012)
794 is needed to determine when (and in what extent) the average of the biological response does
795 not match the response to the average temperature. In all those cases quantitative predictions
796 are not those expected from intuition. The approach presented here deals with non-linearities
797 and interactive responses to the predictors (as above), and non-linear transformations between
798 different frames. For example, the solutions of partial differential equations can help us to
799 identify scenarios when the type of multiple driver response depends on the metrics of time

800 (worked example, Fig. 9 and Giménez et al. 2022). Given only two components of a single
801 fluctuation (magnitude and time scale) we can still rely on 2D graphical representations for a
802 better understanding of a response depends on the coordinate frames, as illustrated Figure 3
803 (i.e. the response on different surfaces). However, in cases of two or more fluctuations (e.g.
804 temperature plus a second environmental variable) the responses will lie on higher dimensional
805 surfaces and intuition will be of limited help. It seems to me that, as the field progresses, the
806 stronger mathematical emphasis will constitute an important guide to navigate through the
807 complexity of high dimensional phenomena, interactive effects and non-linearities. Hence, the
808 mathematical analysis used here, may be considered an additional step in the processes
809 summarised in Figure 2, helping with the design and interpretation of experiments as well as
810 the application scale transition.

811 SOFiA incorporates the biological perspective, defined by the time scale and the capacity of
812 organisms and other biological systems to cope with environmental fluctuations. The first
813 important concept is the “region of existence”, defined from fixed values of μ and τ (both set
814 to 1 in the example). This is an important point in the light of discussions concerning the
815 definition of heatwaves (Baley and Van de Pol 2015, Hobday et al, 2016, Jacox 2019). From
816 the biological standpoint, heatwaves would be defined as the set of extreme fluctuations
817 (characterised by $\mu = 1$), which depend on the time scale of the fluctuation. Many studies show
818 that tolerance to a given stressor scale with the inverse of the logarithm of the time of exposure
819 (revision in Rezende et al. 2014). Such biological definition would incorporate the rescue effect
820 produced by adaptive plasticity. Simulations in Case 3 highlight the importance of time delays
821 in the expression of the plastic response in determining the set of extreme fluctuations.

822 The starting point in SOFiA was to consider fluctuations as a collection of components (as in
823 Hobday et al. 2016) and defining fluctuations as objects existing in an hypervolume, in the
824 same way that ecologists define elements in the ecological niche (Blonder 2018) or characterise
825 communities (e.g. Legendre & Legendre 2008). At the organismal level, the space of
826 fluctuations has connections with the concept of tolerance landscape (Rezende et al. 2014)
827 where the response is tolerance, as existing within a space defined by the magnitude and time
828 scale of exposure to a particular stressor. At the species level, there are connections with the
829 Hutchinson view of the niche (i.e. where resources or environmental variables define the axes),
830 but adding time variables, and meeting the needs of incorporating phenology into the concept
831 of the niche (see Ponti & Sanolo 2022). In addition, for both cases, the main contribution of

832 SOFiA is the quantification of the perspective of organisms through additional reference
833 frames.

834 Different perspectives, including that of the observer, are related through mapping functions
835 (from t to τ and m to μ). We can also consider a case with two different frames representing
836 two different species; in such a case, we can remove the reference frame of the human observer
837 from the equations (see Supplement: Section 7) and project the response of the first species
838 from the perspective of second one. The framework can also be used to visualise biological
839 responses underpinned by different mechanisms (or based on empirical fits) of how tolerance
840 and biological time respond to a given fluctuation. For example, the comparison among cases
841 1- 3 helps to identify properties that are contingent on the presence of plasticity or the adoption
842 of a specific type of trade-off between critical temperature of tolerance period. In addition to
843 the metabolic theory of ecology, the response of developmental time has been predicted from
844 theory or other equations (Ahlgren 1987, Guerrero et al. 1994, McLaren 1995, Shi et al. 2016,
845 Quinn 2021).

846 In SOFiA, the rescue effect of adaptive plasticity (Windig et al. 2004, Chevin et al. 2010) is
847 expressed as the expansion the region of existence (where effects of fluctuations on invariants
848 are buffered). In the simulation, the expansion occurred at intermediate time scales because
849 short term thermal fluctuations were not enough to sustain rapid phenotypic change.
850 Expansions of the space of existence at shorter (or longer) time scales should be based on the
851 concerted action of plastic responses operating at different time scales, i.e. from hardening to
852 long term acclimation (Donelson et al. 2011). Hence, the simulation shows that better
853 understanding of the responses to fluctuations requires models of the “dynamics” of the
854 formation of the phenotype, which instead will depend on the scale-dependent plastic response.
855 Such models require experiments quantifying how the rate of phenotypic change experienced
856 by an organism is driven by temperature; central to such research are time keeping mechanisms
857 (Giménez et al. 2022) and metabolic rates (Jackson et al. 2021).

858 An important point in SOFiA is to differentiate between invariants (e.g. body mass) and rates
859 (e.g. growth or sensitivity). Rates capture the relative aspect of the “effect” of a fluctuation on
860 the invariant because they depend on the reference frame. Hence, SOFiA introduces a level of
861 “relativism” in the nature of the responses to stressors. This is particularly important when
862 more than one stressor is considered. In such a case, the type of frame (intrinsic or extrinsic)
863 determines the nature of the interactive effect of two stressors on an invariant response

864 (Giménez et al. 2022). An important example concerns the combined effect of increased
865 temperature and a second environmental variable. For instance, because temperature increases
866 metabolic demands, increased temperature can exacerbate the negative effect of food limitation
867 on body reserves to metamorphosis (Torres & Giménez 2020). In addition, increased
868 temperature can either mitigate or exacerbate the effect of reduced salinity on survival to
869 metamorphosis (Torres et al. 2021). Importantly, because thermal fluctuations drive
870 developmental rates, the magnitude of body size responses can be only expressed as relative to
871 the reference frame used to measure time. The relativism introduced here has implications for
872 multiple stressor research; for instance, additive effects relative to the clock time will become
873 interactive in biological time (Giménez et al. 2022). Multiple stressor research has been
874 motivated by the recognition that climate change affects several environmental variables at a
875 time (Gunderson et al. 2016, Boyd et al. 2018). An important objective of this field involves
876 the quantification of the frequency of occurrence of the different types of interactive effects
877 and in which context a stressor mitigates or enhances the effect of another stressor. The fact
878 that the nature of the multiple stressor effect can depend on the reference frame highlights the
879 need to be clear about what is the relevant frame to address a given question.

880 **5.1 Wider applications**

881 I argue that SOFiA is a general approach in the following sense. First, it can be applied in
882 situations where biological time and tolerance do not depend on the fluctuations or to more
883 complex experimental designs. If biological time and tolerance do not depend on the
884 fluctuation, the partial differential equation 2 simplifies such that the matrix M contains zero's
885 in the off-diagonal entries (μ and τ become linearly related to m and t respectively) and the
886 response is projected on 2D flat time slices (Fig 3) at both clock and biological time. Second,
887 given a single variable (e.g. temperature), one can apply this approach to experiments exploring
888 the effect of consecutive waves on biological variables responses, by adding a component (to
889 the space of fluctuations) quantifying the time lag between waves (called respectively l and λ
890 in the extrinsic and intrinsic frames). Third, one can accommodate additional variables (e.g.
891 food availability, salinity, pCO_2) and the time lag among them, in order to explore the effect of
892 simultaneous vs sequential stressor effects (Gunderson et al. 2016). As the level of complexity
893 increases, the limitations are logistical; however, in such a case, one could use information
894 from previous experiments and the mathematical formalism to determine which region of the
895 space of fluctuations should be further explored through a new experiment. Fourth, SOFiA can

896 be applied beyond the organismal level, if one can define metrics for biological times and
897 tolerance (discussion below).

898 A potential application concerns the species level, where tolerance may be defined as the
899 thermal range enabling positive population growth rate (Gvozdk 2018) and biological time is
900 defined as the generation time. Given two species, we have species-specific biological time
901 scales (τ_1, τ_2) and amplitudes (μ_1, μ_2). In the mt-projection, the area where both μ_1 and $\mu_2 > 1$
902 are regions of extinction for both species. The regions where only one of them is > 1 , shows
903 extinction of only one such species; interactions such as symbiosis would be reflected as $\mu_1 =$
904 μ_2 . Areas where any $\mu_i > 1$ indicate conditions leading to environmental filtering (Kraft et al.
905 2014) where temperature selects for species assemblages characterised by specific traits
906 combinations. How $\mu_i = 1$ curves are positioned with respect to $\tau_i = 1$ curves will define regions
907 where extreme fluctuations are longer/shorter than the generation times. Theory (Romero-
908 Mujalli et al. 2021) predicts that the threshold of $\tau = 1$ is important for how adaptive plasticity
909 responds to fluctuations over long time scales.

910 Portfolio effects (Schindler et al. 2015), driven by phenotypic plasticity and genetic diversity,
911 buffer populations from environmental fluctuations. Portfolio effects should result in patterns
912 analogous to those of Figure 8, which contrast to those shown in Figure 7. There are also
913 outcomes that depend on the type of interaction. In case of competition, relative nonlinearity
914 and storage effects maintain coexistence under environmental fluctuations (Descamp-Julien &
915 Gonzalez 2005, Chesson 2018); fluctuations of sufficiently low amplitude should result in
916 competitive exclusion, unless fluctuation independent mechanisms operate. Fluctuation-
917 dependent mechanisms may be reflected in μ -values if “tolerance” is quantified considering
918 the outcome of species interactions.

919 The second case concerns biodiversity and ecosystem function (Garcia et al. 2018), where the
920 invariant function would be biomass or the amount of habitat produced by a foundation species.
921 Examples are macroalgal or mussel beds and coral reefs sustaining function in association to
922 its biomass or canopy. Increases in temperature lead to e.g. coral bleaching (Pratchett et al.
923 2008). Here, the curve $\tau = 1$ would represent fluctuations occurring at the time scale of the
924 species replacement (i.e. a metric of biological time unit at the level of community: Ontiveros
925 et al. 2021). Community tolerance is defined from the sensitivity of species richness to changes
926 in the time scale of the fluctuation. By moving along the line of $\mu = 1$, we can identify the set
927 of environmental fluctuations driving extinction and collapsing the function. The absence of

928 buffering mechanisms should result in patterns like Figure 7. Buffer effects (as plasticity in
929 Fig. 8) will reflect phenotypic plasticity, portfolio, or storage effects. In addition, at this level,
930 species complementarity should also operate as a buffer; species complementarity can sustain
931 function in scenarios of increased temperature (Garcia et al. 2018).

932 In synthesis, SOFiA could help to advance our understanding and to predict effects of
933 environmental fluctuations on biological systems. This is achieved through the synthesis,
934 organisation, and re-interpretation of current information about effects of environmental
935 fluctuations on tolerance, biological time and chosen “invariant” responses. As a perspective,
936 SOFiA offers a route for future research, combining a mathematical analysis, simulations and
937 experiments (manipulating fluctuation components) which are then integrated in a wider
938 research programme.

939 REFERENCES

940 Abram, PK, Boivin G, Moiroux J, Brodeur J (2017) Behavioural effects of temperature on
941 ectothermic animals: unifying thermal physiology and behavioural plasticity. *Biol Rev* 92:
942 1859–1876.

943 Ahlgren G (1987) Temperature functions in biology and their application to algal growth
944 constants. *Oikos* 49:177–190.

945 Angilletta MJ (2009) *Thermal adaptation: a theoretical and empirical synthesis*. Oxford.

946 Bailey LD, van de Pol M (2016). Tackling extremes: challenges for ecological and
947 evolutionary research on extreme climatic events. *J Anim Ecol* 85:85–96.

948 Benedetti-Cecchi L (2003) The importance of variance around the mean effect size of
949 ecological processes. *Ecology* 84: 2335–2346.

950 Benedetti-Cecchi L (2021) Complex networks of marine heatwaves reveal abrupt transitions
951 in the global ocean. *Sci Rep* 11:1739.

952 Benedetti-Cecchi L, Bertocci I, Vaselli S, Maggi E (2006). Temporal variance reverses the
953 impact of high mean intensity of stress in climate experiments. *Ecology* 87:2489–2499.

954 Bernhardt JR, O'Connor MI, Sunday JM, Gonzalez A (2020) Life in fluctuating
955 environments. *Phil Trans R Soc B* 375:20190454.

956 Bertoci I, Vaselli S, Maggi E, Benedetti-Cecchi, L (2007) Changes in temporal variance of
957 rocky shore organism abundances in response to manipulation of mean intensity and temporal
958 variability of aerial exposure. *Mar Ecol Prog Ser* 338:11-20.

959 Bigelow WD (1921). The logarithmic nature of thermal death time curves. *J Infectious*
960 *Diseases* 29:528–536.

961 Blonder B (2018). Hypervolume concepts in niche- and trait-based ecology. *Ecography* 41:
962 1441–1455.

963 Box GEP, Wilson KB (1951). On the experimental attainment of optimum conditions. *J R*
964 *Stat Soc B* 13:1–38.

965 Boyd PW, Collins S, Dupont S, Fabricius K, Gattuso J-P, Havenhand J, Hutchins DA,
966 Riebesell U, Rintoul MS, Vichi M, Biswas H, Ciotti A, Gao K, Gehlen M, Hurd K, Kurihara
967 H, McGraw KM, Navarro JM, Nilsson GE, Pasow U, Pörtner H-O (2018). Experimental
968 strategies to assess the biological ramifications of multiple drivers of global ocean change—A
969 review. *Glob Change Biol* 24:2239–2261.

970 Brown JH, Gillooly JF, Allen AP, Savage M, West GB (2004). Towards a metabolic theory
971 of ecology. *Ecology* 85:771–1789.

972 Buoro M, Giménez O, Prévost E (2012). Assessing adaptive phenotypic plasticity by means
973 of conditional strategies from empirical data: the latent effect threshold model. *Evolution*
974 66:996–1009.

975 Burraco P, Orizaola G, Monaghan P, Metcalfe NB (2020) Climate change and ageing in
976 ectotherms. *Glob Change Biol* 26:5371–5381.

977 Cadotte MW (2013). Experimental evidence that evolutionarily diverse assemblages result in
978 higher productivity. *Proc Natl Acad Sci USA* 110:8996–9000.

979 Cayuela H, Lemaître JF, Muths E, McCaffery RM, Fretey T, le Garff B, Schmidt BR,
980 Grossenbacher K, Lenzi O, Hossack BR, Eby LA, Lambert BA, Elmberg J, Merila J, Gippet
981 JMW, Gaillard JM, Pilliod DS (2021). Thermal conditions predict intraspecific variation in
982 senescence rate in frogs and toads. *Proc Natl Acad Sci US* 118:e2112235118.

983 Chave J (2013). The problem of pattern and scale in ecology: what have we learned in 20
984 years? *Ecol. Lett* 16:4–16.

985 Chesson P (2018). Updates on mechanisms of maintenance of species diversity. *J Ecol* 106:
986 1773-1794.

987 Chevin LM, Lande R, Mace GM (2010). Adaptation, plasticity, and extinction in a changing
988 environment: towards a predictive theory. *PLoS Biol* 8:e1000357.

989 Cottingham KL, Lennon JT, Brown BL (2005). Knowing when to draw the line: designing
990 more informative ecological experiment. *Frontiers Ecol Environ* 3:145–152.

991 Dal Bello M, Rindi L, Benedetti-Cecchi L (2017). Legacy effects and memory loss: how
992 contingencies moderate the response of rocky intertidal biofilms to present and past extreme
993 events. *Glob Change Biol* 23:3259–3268.

994 Dawirs RR (1985) Temperature and larval development of *Carcinus maenas* (Decapoda) in
995 the laboratory; predictions of larval dynamics in the sea *Mar Ecol Prog Ser* 24: 297–302.

996 Dawson TP, Jackson S, House J, Prentice IC, Mace GM (2011). Beyond predictions:
997 biodiversity conservation in a changing climate. *Science* 332:53–58.

998 De Laender F (2018). Community- and ecosystem-level effects of multiple environmental
999 change drivers: Beyond null model testing. *Glob Change Biol* 24:5021–5030.

1000 DeRivera C, Hitchcock NG, Teck SJ, Steves BP, Hines AH, Ruiz GM (2007) Larval
1001 development rate predicts range expansion of an introduced crab. *Mar Biol* 150: 1275–1288.

1002 DeWitt TJ, Sih A, Wilson DS (1998). Costs and limits of phenotypic plasticity. *Trends Ecol*
1003 *Evol*, 13:77–81.

1004 Denny M (2019) Performance in a variable world: using Jensen’s inequality to scale up from
1005 individuals to populations. *Conserv Physiol* 7:coz053. 1.

1006 Denny M, Benedetti-Cecchi L (2012) Scaling up in ecology: Mechanistic approaches. *Annu*
1007 *Rev. Ecol Evol Syst* 43:1–22.

1008 Descamps-Julien B, Gonzalez A (2005). Stable coexistence in a fluctuating environment: an
1009 experimental demonstration. *Ecology* 86:2815–2824.

1010 Donelson JM, Salinas S, Munday PL, Shama LNS (2018). Transgenerational plasticity and
1011 climate change experiments: Where do we go from here? *Glob Change Biol* 24:13–34.

1012 Dowd WW, King FA, Denny MW (2015) Thermal variation, thermal extremes and the
1013 physiological performance of individuals. *J Exp Biol* 218:1956–1967.

1014 Fraterrigo JM, Rusak JA (2008) Disturbance-driven changes in the variability of ecological
1015 patterns and processes. *Ecol Lett* 11:756–770.

1016 García FC, Bestion, E, Warfield R, Yvon-Durocher G (2018). Changes in temperature alter
1017 the relationship between biodiversity and ecosystem functioning. *Proc Natl Acad Sci USA*,
1018 115:10989–10994.

1019 Gerhard M, Koussoroplis AM, Raatz M, Pansch C, Fey SB, Vajedsamiei J, Calderó-Pascual
1020 M, Cunillera-Montcusí D, Juvigny-Khenafou NPD, Polazzo F, Thomas PK, Symons CC,
1021 Beklioglu M, Berger SA, Chefaoui RM, Ger KA, Langenheder S, Nejstgaard JC, Ptacnik R,
1022 Striebel M (2023) Environmental variability in aquatic ecosystems: Avenues for future
1023 multifactorial experiments. *Limnol Oceanogr Letters* 8:247–266.

1024 Gerken AR, Eller OC, Hahn, DA, Morgan TJ (2015). Constraints, independence, and
1025 evolution of thermal plasticity: Probing genetic architecture of long- and short-term thermal
1026 acclimation. *Proc Natl Acad Sci USA* 112:4399–4404.

1027 Gillooly JE, Charnov EL, West GB, Savage VM, Brown JH (2002) Effects of size and
1028 temperature on developmental time. *Nature* 417:70–71.

1029 Giménez L, 2006. Phenotypic links in complex life cycles: conclusions from studies with
1030 decapod crustaceans. *Int Comp Biol* 46, 615–622.

1031 Giménez L (2011). Exploring mechanisms linking temperature increase and larval
1032 phenology: The importance of variance effects. *J Exp Mar Biol Ecol* 400: 227–235.

1033 Giménez L (2020) Phenotypic plasticity and phenotypic links in larval development. Chapter
1034 13 in Thiel M, Anger K, Harzsch S, Chapter in *Larval Biology*; Volume 7 of Series: The
1035 Natural History of the Crustacea. Oxford

1036 Giménez L, Chatterjee A, Torres G (2021). A state-space approach to understand responses
1037 of organisms, populations and communities to multiple environmental drivers. *Comms Biol*
1038 4:1142.

1039 Giménez L, Espinosa N, Torres G (2022). A framework to understand the role of biological
1040 time in responses to fluctuating climate drivers. *Sci Rep* 12:10429.

1041 Gunderson A, Armstrong E, Stillman J (2016) Multiple stressors in a changing world: the
1042 need for an improved perspective on physiological responses to the dynamic marine
1043 environment. *Annu Rev Mar Sci* 8:357–378.

1044 Guerrero F, Blanco JM, Rodríguez V (1994) Temperature-dependent development in marine
1045 copepods: a comparative analysis of models. *J Plankton Res* 16: 95-103.

1046 Gvoždík L (2018). Just what is the thermal niche? *Oikos* 127:1701–1710.

1047 Hazel WN, Smock R, Johnson MD (1990). A polygenic model for the evolution and
1048 maintenance of conditional strategies. *Proc R Soc B* 242:81–187.

1049 Hobday AJ, Alexander LV, Perkins SE, Smale DA, Straub SC, Oliver ECJ Benthuisen JA,
1050 Burrows MT, Donat MG, Feng M, Holbrook NJ, Moore P Scannell HA, Gupta AS,
1051 Wernberg T . (2016). A hierarchical approach to defining marine heatwaves. *Prog Oceanogr*
1052 141:227–238.

1053 Hoffmann AA, Sorensen JG, Loeschke V (2003). Adaptation of *Drosophila* to temperature
1054 extremes: bringing together quantitative and molecular approaches. *J Therm Biol* 28:175.

1055 Jackson MC, Pawar S, Woodward, G. (2021) Temporal dynamics of multiple stressor effects:
1056 from individuals to ecosystems. *Trends Ecol Evol* 36:402–410.

1057 Jacox MG (2019). Marine heatwaves in a changing climate. *Nature* 571:485–486.

1058 Jørgensen LB, Malte H, Overgaard J (2019). How to assess *Drosophila* heat tolerance:
1059 Unifying static and dynamic tolerance assays to predict heat distribution limits. *Funct Ecol*
1060 33:629–642.

1061 Koussoroplis AM, Pincebourde S, Wacker A (2017) Understanding and predicting
1062 physiological performance of organisms in fluctuating and multifactorial environments. *Ecol*
1063 *Monogr* 87: 178–197.

1064 Kreyling J, Jentsch A, Beier C (2014). Beyond realism in climate change experiments:
1065 gradient approaches identify thresholds and tipping points. *Ecol Lett* 17:125–e1.

1066 Kreyling J, Schweiger AH, Bahn M, Ineson P, Migliavacca M, Morel-Journel T, Christiansen
1067 JR, Schtickzelle N, Larsen KS (2018). To replicate, or not to replicate – that is the question:
1068 how to tackle nonlinear responses in ecological experiments. *Ecol Lett* 21:629–1638.

1069 Kroeker KJ Bell LE, Donham EM, Hoshijima U, Lummis S, Toy J, Willis-Norton E (2020)
1070 Ecological change in dynamic environments: Accounting for temporal environmental
1071 variability in studies of ocean change biology. *Glob Change Biol.* 26: 54–67.

1072 Laubach ZM, Holekamp KE, Aris, IM, Slopen N, Perng W (2022). Applications of
1073 conceptual models from lifecourse epidemiology in ecology and evolutionary biology. *Biol*
1074 *Lett* 18:20220194.

1075 Legendre P, Legendre L (2012). *Numerical Ecology*. Elsevier.

1076 Levins R (1968) *Evolution in changing environments: some theoretical explorations*.
1077 *Monographs in Population Biology* 2. Princeton.

1078 Lynch HJ, Rhainds M, Calabrese JM, Cantrell, S, Cosner C, Fagan WF (2014). How climate
1079 extremes-not means- define a species' geographic range boundary via a demographic tipping
1080 point. *Ecol Monogr* 84:131–149.

1081 Maggi E, Bulleri F, Bertocci I, Benedetti-Cecchi L (2012). Competitive ability of macroalgal
1082 canopies overwhelms the effects of variable regimes of disturbance. *Mar Ecol Prog Ser*
1083 465:99–109

1084 Manenti T, Loeschcke V, Sørensen JG (2018). Constitutive up-regulation of *Turandot* genes
1085 rather than changes in acclimation ability is associated with the evolutionary adaptation to
1086 temperature fluctuations in *Drosophila simulans*. *J Insect Physiol* 104:40–47.

1087 Marshall DJ, Burgess SC, Connallon T (2016). Global change, life-history complexity and
1088 the potential for evolutionary rescue. *Evol Appl* 9:1189–1201.

1089 McLaren I (1995) Temperature-dependent development in marine copepods: comment on
1090 choices of models. *J Plankton Res* 17: 1385–1390.

1091 Minuti JJ, Byrne M, Campbell H, Hemraj DA, Russell BD (2022). Live-fast-die-young:
1092 Carryover effects of heatwave-exposed adult urchins on the development of the next
1093 generation. *Glob Change Biol* 28:5781–5792.

1094 Munch SB, Rogers TL, Symons CC, Pennekamp F (2023) Constraining nonlinear time series
1095 modeling with the metabolic theory of ecology. *Proc Natl Acad Sci USA* 120:e2211758120.

1096 Needham T (2021) *Visual differential geometry and forms*. Princeton University Press.

1097 Niehaus AC, Angilletta MJ, Sears MW, Franklin CE, Wilson RS (2012). Predicting the
1098 physiological performance of ectotherms in fluctuating thermal environments. *J Exp Biol*
1099 215:694–701.

1100 Pechenik J (2006). Larval experience and latent effects—metamorphosis is not a new
1101 beginning, *Integr Comp Biol* 46:323–333.

1102 Pörtner HO, Schulte PM, Wood CM, Schiemer F (2010). Niche dimensions in fishes: An
1103 Integrative View. *Physiol Biochem Zool* 83:808–826.

1104 Pratchett MS, Munday PL, Wilson SK, Graham NA, Cinner JE, Bellwood DR, Jones JP,
1105 Polunin NV, McClanahan TR (2008) Effects of climate -induced coral bleaching on coral
1106 reef fishes – ecological and economic consequences. *Oceanogr Mar Biol Annu Rev* 48: 251–
1107 296.

1108 Ontiveros VJ, Capitán JA, Casamayor EO, Alonso D (2021). The characteristic time of
1109 ecological communities. *Ecology* 102:e03247.

1110 Ponti R, Sannolo M (2022). The importance of including phenology when modelling species
1111 ecological niche. *Ecography* e06143.

1112 Pörtner HO (2002). Climate variations and the physiological basis of temperature dependent
1113 biogeography: systemic to molecular hierarchy of thermal tolerance in animals. *Comp*
1114 *Biochem Physiol A* 132:739–761.

1115 Quinn BK (2021). Performance of the SSI development function compared with 33 other
1116 functions applied to 79 arthropod species’ datasets. *J Thermal Biol* 102:103–112.

1117 Reid JM, Acker P (2022). Properties of phenotypic plasticity in discrete threshold traits.
1118 *Evolution* 76:190–206.

1119 Rezende EL, Castañeda LE, Santos M (2014). Tolerance landscapes in thermal ecology.
1120 *Funct Ecol* 28:799–809.

1121 Roman & Pierson 2022,

1122 Rombough P (2003) Modelling developmental time and temperature. *Nature* 424:268–269

1123 Romero-Mujalli D, Rochow M, Kahl S, Paraskevopoulou S, Folkertsma R, Jeltsch F, *et al.*
1124 (2021). Adaptive and nonadaptive plasticity in changing environments: Implications for
1125 sexual species with different life history strategies. *Ecol Evol* 11:6341–6357.

1126 Ruiz-Herrera A (2017). Carry-over effects: population abundance, ecological shifts, and the
1127 (dis-)appearance of oscillations. *Ecol Mod* 349:26–32.

1128 Russo S, Sillmann J, Fischer EM (2015). Top ten European heatwaves since 1950 and their
1129 occurrence in the coming decades. *Environ Res Lett* 10:124003.

1130 Sæther B-E, Engen S (2015). The concept of fitness in fluctuating environments. *Trends Ecol*
1131 *Evol* 30:273–281.

- 1132 Salachan PV, Sørensen JG (2022). Molecular mechanisms underlying plasticity in a
1133 thermally varying environment. *Molec Ecol* 31:3174–3191.
- 1134 Rezende EL, Santos M (2012). Comment on ‘Ecologically relevant measures of tolerance to
1135 potentially lethal temperatures’ *Exp Biol* 215:702–703.
- 1136 Šargač Z, Giménez L, González-Ortegón E, Harzsch S, Tremblay N, Torres G (2022)
1137 Quantifying the portfolio of larval responses to salinity and temperature in a coastal-marine
1138 invertebrate: a cross population study along the European coast. *Mar Biol* 169:81
- 1139 Scheiner SM (2016). Habitat choice and temporal variation alter the balance between
1140 adaptation by genetic differentiation, a jack-of-all-trades strategy, and phenotypic plasticity.
1141 *Am Nat* 187:633–646.
- 1142 Schweiger AH, Irl SDH, Steinbauer MJ, Dengler J, Beierkuhnlein C (2016). Optimizing
1143 sampling approaches along ecological gradients. *Methods Ecol Evol* 7: 463–471.
- 1144 Seebacher F, Beaman J, Little AG (2014). Regulation of thermal acclimation varies between
1145 generations of the short-lived mosquitofish that developed in different environmental
1146 conditions. *Funct Ecol* 28:137–148.
- 1147 Schindler DE, Armstrong JB, Reed TE (2015). The portfolio concept in ecology and
1148 evolution. *Front Ecol Environ* 13:257–263.
- 1149 Shi P-J, Reddy GVP, Chen L, Ge F (2016). Comparison of thermal performance equations in
1150 describing temperature-dependent developmental rates of insects: (II) Two Thermodynamic
1151 Models. *Ann Entom Soc America* 110:113–120.
- 1152 Smith MD (2011). An ecological perspective on extreme climatic events: a synthetic
1153 definition and framework to guide future research. *J Ecol* 99:656-663.
- 1154 Stearns S (1986). *Evolution of life histories*. Oxford Univ Press.
- 1155 Tang J, Ikediala JN, Wang S, Hansen JD, Cavalieri RP (2000). High-temperature-short-time
1156 thermal quarantine methods. *Postharvest Biol Technol* 21:129–145.
- 1157 Terblanche JS, Hoffmann AA, Mitchell KA, Rako L, le Roux PC, Chown SL (2011).
1158 Ecologically relevant measures of tolerance to potentially lethal temperatures. *J Exp Biol*
1159 214:3713–3725.
- 1160 Thompson RM, Beardall J, Beringer J, Grace M, Sardina P (2013) Means and extremes:
1161 building variability into community-level climate change experiments. *Ecol Lett* 16:799–806.

1162 Torres G, Giménez L (2020). Temperature modulates compensatory responses to food
1163 limitation at metamorphosis in a marine invertebrate. *Funct Ecol* 34:1564–1576.

1164 Torres G, Charmantier G, Wilcockson D, Harzsch S, Giménez L (2021) Physiological basis
1165 of interactive responses to temperature and salinity in coastal marine invertebrate:
1166 Implications for responses to warming. *Ecol Evol* 11:7042–7056.

1167 Torres G, Giménez L, Pettersen AK, Bue M, Burrows MT, Jenkins SR (2016) Persistent and
1168 context-dependent effects of the larval feeding environment on post-metamorphic
1169 performance through the adult stage. *Mar Ecol Prog Ser* 545:147–160.

1170 Turner MG, Romme WH, Gardner RH, Oneill RV, Kratz TK (1993) A revised concept of
1171 landscape equilibrium: disturbance and stability on scaled landscapes. *Landsc Ecol* 8:213–
1172 227.

1173 Uller T, Nakagawa S, English S (2013) Weak evidence for anticipatory parental effects in
1174 plants and animals. *J Evol Biol*, 26, 2161–2170.

1175 Urban HJ (1994) Upper temperature tolerance of ten bivalve species off Peru and Chile
1176 related to El Nino. *Mar Ecol Prog Ser* 107: 139–145.

1177 Vasseur DA, Yodzis P (2004) The color of environmental noise. *Ecology* 85:1146–1152.

1178 Vinebrooke D, Cottingham RL, Norberg K, Scheffer M, Dodson JI, Maberly SC, Sommer U
1179 (2004). Impacts of multiple stressors on biodiversity and ecosystem functioning: the role of
1180 species co-tolerance. *Oikos* 104:451-457.

1181

1182